Chinese Journal of
POLYMER SCIENCE

REVIEW

https://doi.org/10.1007/s10118-025-3550-0
Chinese J. Polym. Sci.

Design, Synthesis, and Photocatalytic Applications of sp^2-Carbon-Conjugated Organic Frameworks

Meng-Yao Chen[a,b], Guang-En Fu[a,c], Wen-Kai Zhao[a,b], and Tao Zhang[a*]

[a] *Ningbo Institute of Materials Technology & Engineering, Chinese Academy of Sciences, State Key Laboratory of Advanced Marine Materials, Ningbo 315201, China*
[b] *University of Chinese Academy of Sciences, Beijing 100049, China*
[c] *Key Laboratory of Biomass Chemical Engineering of Ministry of Education, College of Chemical and Biological Engineering, Zhejiang University, Hangzhou 310027, China*

Abstract sp^2-Carbon-conjugated organic frameworks (sp^{2}c-COFs) are a class of porous crystalline polymers constructed through the ordered linkage of building blocks *via* vinylene bonds. Because of their high specific surface area, extended planar π-conjugation, and remarkable stability, sp^{2}c-COFs are regarded as highly promising novel photocatalysts. This review begins by introducing the design principles and synthetic methods for sp^{2}c-COFs. Subsequently, various strategies for enhancing photocatalytic performance have been summarized, including designing donor-acceptor (D-A) structures, crafting charged frameworks, developing heterojunctions, and modifying covalent organic frameworks (COFs) pore channels. We then elaborate on the applications of sp^{2}c-COFs in photocatalytic H_2 production, H_2O_2 production, CO_2 reduction, organic transformation reactions, and uranium extraction from seawater. Finally, the challenges and future prospects of sp^{2}c-COFs for practical applications in photocatalysis were discussed.

Keywords Covalent organic frameworks (COFs); sp^2-Carbon-conjugated; Photocatalysis

Citation: Chen, M. Y.; Fu, G. E.; Zhao, W. K.; Zhang, T. Design, synthesis, and photocatalytic applications of sp^2-carbon-conjugated organic frameworks. *Chinese J. Polym. Sci.* https://doi.org/10.1007/s10118-025-3550-0

1 INTRODUCTION

The rapid development of the industrial society has led to the accelerated depletion of fossil fuels, resulting in severe ecological damage and an energy crisis.[1–3] The development of clean and renewable energy has become an urgent priority for the sustainable development of human society. Solar energy is an inexhaustible green energy source. Selecting suitable photocatalysts to convert green solar energy into useful chemical energy is a crucial approach for addressing the potential energy crisis.[4–8] In 1972, Fujishima and Honda achieved photolysis of water into hydrogen and oxygen using TiO_2 under UV light, which marked a breakthrough in the field of photocatalysis.[9] For decades, photocatalytic technology has been extensively studied and applied in various fields, including photocatalytic H_2 production,[10–12] H_2O_2 production,[13–15] CO_2 reduction,[16–18] organic transformation reactions,[19] and pollutant degradation.[20,21] However, traditional semiconductor photocatalytic materials such as TiO_2, CdS, and g-C_3N_4 often suffer from drawbacks such as narrow light absorption ranges, high carrier recombination rates, and poor stability, which limit their overall photocatalytic efficiency.[22–27] Therefore, the development of novel photocatalytic materials to efficiently harness and convert solar energy for future practical applications is of great scientific importance and broad application prospects.

Covalent organic frameworks (COFs) are porous crystalline polymers formed by ordered covalent linkage of molecular units *via* reversible reactions.[28,29] Since Yaghi reported the first boronate ester-linked COFs in 2005,[30] these materials have attracted significant attention from researchers because of their ordered porous structures, diverse types of linking

* Corresponding author, E-mail: tzhang@nimte.ac.cn
Special Topic: Porous Polymers
Received November 25, 2025; Accepted December 27, 2025; Published online April 3, 2026

bonds, and high structural designability. Compared to traditional inorganic catalytic materials, COFs not only exhibit the typical characteristics of porous materials, such as high specific surface area and low density, but also possess unique advantages, including flexible topological structures, tunable microporosity, and numerous functionalization sites,[31–35] which make them have broad application potential in the field of photocatalysis.

In 2016, Feng and Zhang *et al*. developed the first carbon-carbon double bond-linked sp^2c-COFs (2DPPV) through the Knoevenagel reaction.[36] Unlike non-conjugated boronic ester bonds and non-fully conjugated imine bonds, sp^2c-COFs exhibit outstanding structural stability and charge carrier mobility,[37–39] demonstrating significant advantages in the field of photocatalysis. The porous structure of COFs exposes a large number of reactive sites, which not only promotes mass transfer, but also accelerates the rate of redox reactions. The well-defined chemical composition of COFs offers an exceptional design flexibility. Through monomer structure design or simple post-modification, the optoelectronic properties of COFs can be precisely tuned to match the diverse application scenarios. In addition, the unique fully conjugated backbone of sp^2c-COFs provides extended π-delocalized conjugation, offering a high-speed pathway for the separation and migration of photogenerated carriers and effectively inhibiting the recombination of electron-hole pairs. C=C double bonds are resistant to hydrolysis and maintain exceptional structural stability even under strongly acidic or alkaline conditions, enabling long-term stable operation in complex photocatalytic systems.[40–43]

Although numerous reviews have been published on the synthesis and application of COFs materials, systematic reviews focusing specifically on the photocatalytic progress of sp^2c-COFs remain scarce. In this review, we provide a detailed overview of the design and synthesis strategies for sp^2c-COFs as photocatalysts, along with the latest research advances, with the aim of offering references for the design and synthesis of highly efficient novel sp^2c-COFs photocatalytic materials. We first introduced various organic reactions used for synthesizing sp^2c-COFs, such as the Knoevenagel reaction and aldol reaction. Next, we conducted a detailed discussion on strategies to enhance their photocatalytic performance, including D-A structure design, charged environment construction, heterojunction design, and lattice pore modification. Subsequently, we highlight research advances in sp^2c-COFs as photocatalysts for water splitting hydrogen production, hydrogen peroxide production, carbon dioxide reduction, organic transformation reactions, and uranium extraction from seawater. Finally, we offer forward-looking perspectives on both the opportunities and challenges of sp^2c-COFs, with an eye toward practical implementation and future research directions.

2 DESIGN PRINCIPLES AND SYNTHESIS METHODS FOR SP^2C-COFS

2.1 Design Principles

The sp^2c-COFs possessed a periodically layered framework and remarkable in-plane π-conjugation. Through the design of topological structures, screening of monomer units, and specific chemical reactions, researchers have developed various sp^2c-COFs materials with distinct structures. The monomer units of sp^2c-COFs typically feature both a rigid π-conjugated backbone and at least two reactive functional groups. By controlling the structure, symmetry, reactive groups, and active sites of monomers, common topological structures, such as hexagons, tetragons, triangles, and rhombuses, can be precisely constructed. As shown in Fig. 1(a), hexagonal structures are often obtained through reactions between two C_3 units [C_3+C_3] or between a C_2 unit and C_3 unit [C_2+C_3]. Tetragonal structures can be formed *via* [C_2+C_4] or [C_4+C_4] reactions, whereas trigonal structures result from [C_2+C_6] reactions. For example, Jiang *et al*. constructed rhombic topological sp^2c-COFs by reacting C_2 monomers containing four reactive groups (TFPPy) with C_2 monomers containing two reactive groups (PDAN).[43]

Guided by the topological design principles for the crystal structure of sp^2c-COFs, suitable monomer units were further screened and supplemented with various modification strategies to precisely synthesize specific functionalized sp^2c-COFs. Common building blocks are shown in Fig. 1(b).[44] The aldehyde group can undergo various organic reactions with specific functional groups, such as methyl, activated methylene, and halogens, yielding carbon-carbon double bonds with different orientations. Subtle modifications to the monomer structures and the arrangement of different monomers create millions of potential structures, laying a solid foundation for the structural diversity of sp^2c-COFs.[45,46]

2.2 Synthetic Reaction

In the preparation of sp^2c-COFs, various chemical reactions have been employed to synthesize carbon-carbon double bonds, including the Kovenagel reaction, Aldol reaction, Horner-Wadsworth-Emmons reaction, Claisen-Schmidt reaction, Wittig reaction, and some specific coupling reactions.

The Kovenagel reaction is widely employed to synthesize sp^2c-COFs containing substituents. The electron-withdrawing cyano group activates the adjacent methylene groups. Under the catalysis of a weak base, the activated methylene group undergoes nucleophilic attack on the aldehyde group, further dehydrating to form α,β-unsaturated dicarbonyl compounds (Fig. 1c-i). The research group of Feng and Zhang utilized Cs_2CO_3 to catalyze the Knoevenagel reaction between 1,3,5-tri (4-formylphenyl) benzene (TFPB) and p-phenyleneacetonitrile (PDAN) to develop sp^2c-COFs (2DPPV). 2DPPV presents an AB-stacked laminar serrated structure, featuring a high specific surface area (472 $m^2 \cdot g^{-1}$) and significant crystalline characteristics, demonstrating excellent stability and unique planar charge transport properties.[36] Feng *et al*. investigated the effects of different catalysts on the reaction process. Among catalysts, such as alkali metal carbonates (from Na to Cs), CsF, $BaCO_3$, and NaOH, only Cs_2CO_3 catalysis yielded crystalline two-dimensional sp^2c-COFs with a high yield of 84%. Density functional theory (DFT) calculations indicated that Cs^+ forms a five-membered ring transition state with N and O to stabilize the carbon anion intermediate, thereby establishing a quasi-reversible C—C bond.[47] The Knoevenagel condensation reaction pioneered the synthesis of sp^2c-COFs and significantly expanded the variety of cyano-substituted sp^2c-COFs.

Unlike the Knoevenagel reaction, the aldol reaction occurs between a methyl group activated by an electron-withdrawing group and an aldehyde group. The deprotonated methyl

https://doi.org/10.1007/s10118-025-3550-0

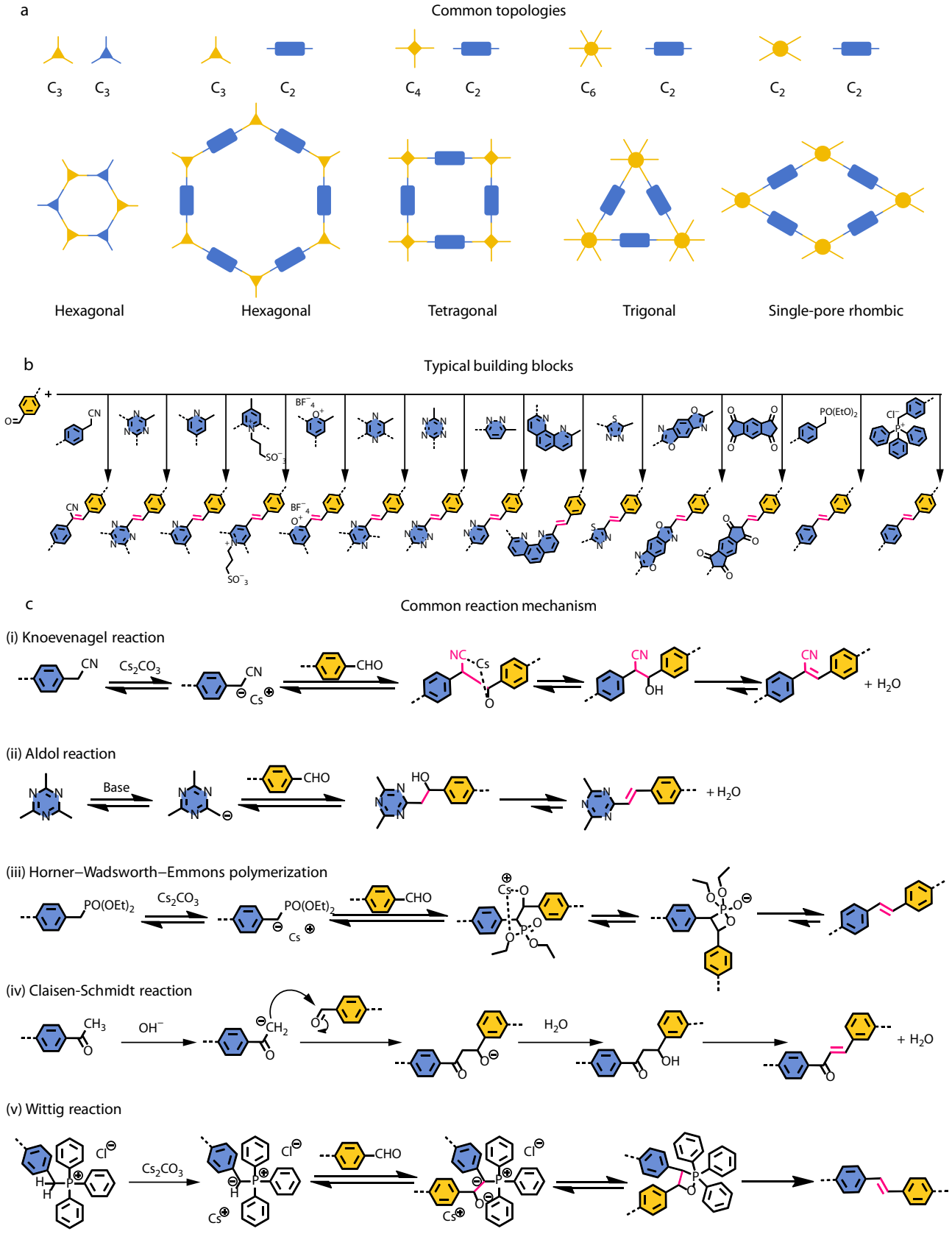

Fig. 1 (a) Schematic diagram of common topological structures of sp^{2}c-COFs; (b) Typical building blocks that can be used to construct sp^{2}c-COFs; (c) Common reactions and mechanisms for synthesizing sp^{2}c-COFs.

https://doi.org/10.1007/s10118-025-3550-0

group forms a reactive carbanion, which acts as a nucleophilic intermediate that attacks the aldehyde group to generate a new C-C bond, and then dehydrates to form unsubstituted sp^2c-COFs (Fig. 1c-ii). Yaghi *et al.* employed the aldol reaction using 2,4,6-trimethyl-1,3,5-triazine (TMT) and 4,4'-biphenyldicarboxaldehyde (BPDA) to synthesize the first unsubstituted sp^2c-COFs (COF-701) in 2019. This framework exhibited high purity, porosity, and crystallinity, demonstrating excellent chemical stability in both strong acids and bases.[30] Additionally, we propose a thiazole-induced aldol condensation strategy that utilizes electron-withdrawing groups such as oxazole, thiazole, thiadiazole, and pyranium ions to activate adjacent methyl groups, mediating the aldol reaction. Using this strategy, we developed a series of highly crystalline sp^2c-COFs exhibiting outstanding photoelectronic activity and efficient charge carrier mobility.[33,40,48–50] The Aldol reaction diversifies the carbon-carbon double bond formation pathways, effectively advancing the development of unsubstituted sp^2c-COFs.

In addition to the two common reactions mentioned above, the Horner-Wadsworth-Emmons reaction (HWE) reaction can be employed to construct sp^2c-COFs (Fig. 1c-iii). Feng *et al.* obtained two triangular topological sp^2c-COFs (2D-PPQV1 and 2D-PPQV2) through the HWE reaction between C_2-symmetric aromatic phosphonic acid and a C_3-symmetric aldehyde monomer under the catalysis of Cs_2CO_3. Subsequent model reactions and DFT calculations indicated that Cs^+ formed a stable six-membered ring transition state, which further formed a reversible C—C bond, ultimately yielding a trans carbon-carbon double bond.[51] The HWE polycondensation reaction provides a straightforward approach for constructing crystalline organic frameworks (MOFs).

Wittig reaction is typically conducted under strongly basic conditions, where aldehyde monomers react with triphenylphosphine lithyl ester (Wittig reagent) to yield alkenes and triphenylphosphine oxide (Fig. 1c-v). Feng *et al.* controlled the selectivity of the Wittig reaction with Cs_2CO_3 and obtained four crystalline sp^2c-COFs with a high E-configuration selectivity. The obtained product had excellent planar conjugation properties and outstanding carrier mobility, demonstrating significant application potential in electronic and optoelectronic devices.[52]

Additionally, reactions such as the Claisen-Schmidt reaction (Fig. 1c-iv) and Heck coupling have also been employed to synthesize sp^2c-COFs.[53,54] However, their applications are relatively limited, and thus will not be detailed here.

3 FUNDAMENTAL PRINCIPLES AND DESIGN STRATEGIES OF COFS-BASED PHOTOCATALYSTS

As a class of porous framework materials with fully conjugated backbones, sp^2c-COFs exhibit ultrahigh surface areas, outstanding thermochemical stability, and unique charge carrier migration pathways. These properties confer a large number of active sites, exceptional charge separation efficiency, and broad application scenarios, endowing sp^2c-COFs with great potential in photocatalysis. To design and optimize novel sp^2c-COFs-based photocatalysts, a thorough understanding of their photocatalytic processes and mechanisms is essential.

3.1 Fundamental Principles of Photocatalysis

The term "photocatalysis" was first proposed in 1921 to describe photochemical processes in plants.[55] However, it was not until 1972 that Fujishima and Honda first used the inorganic semiconductor TiO_2 to achieve photocatalytic water splitting, which gradually became widely known and applied.[9] In recent years, with the continuous advances in experimental exploration and theoretical chemistry techniques, researchers have gradually recognized and elucidated the intrinsic mechanisms of photocatalytic processes. In general, the photocatalytic process can be broadly divided into three main steps (Fig. 2). (1) When the energy of incident photons exceeds the catalyst's bandgap, electrons in the valence band (VB) absorb the photons and transition to the conduction band (CB), leaving holes in the valence band; (2) Electron-hole pairs separate, with some

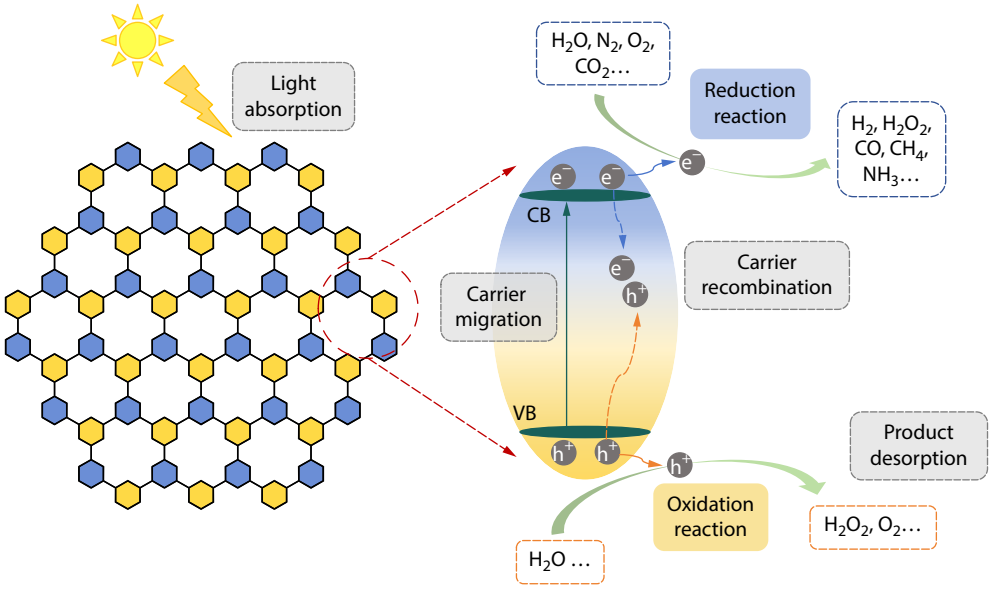

Fig. 2 Schematic diagram of photocatalytic processes on sp^2c-COFs.

migrating along carrier pathways to the catalyst surface, while the remainder recombine within the catalyst; (3) Substrates adsorbed at surface-active sites undergo redox reactions with the electron-hole pairs, desorbing, and releasing products.[56–59] The reaction rates of these three steps collectively determine the overall rate of the photocatalytic reaction.

Therefore, based on the mechanism of photocatalytic reactions, an efficient photocatalyst must satisfy three key requirements: an appropriate bandgap, a high-efficiency charge separation capability, and sufficient surface reactive sites.[40,60] Matching bandgaps (E_g) is a prerequisite for electron-hole pair formation, while appropriate bandgaps can also broaden the light absorption range of the catalyst, thereby enhancing the catalytic performance and improving the light energy utilization efficiency. Carrier separation often relies on the migration pathways within the catalyst. Efficient separation and migration enable more carriers to participate in redox reactions rather than recombine within the catalyst, significantly enhancing catalytic efficiency. Sufficient surface reactive sites enable rapid reactions between the carriers and substrates at multiple sites, thereby accelerating the catalytic reaction process.[61–63]

3.2 Common Strategies for Enhancing the Photocatalytic Performance of COFs

sp^2c-COFs-based photocatalysts can catalyze reactions, including, but not limited to, hydrogen production, hydrogen peroxide production, carbon dioxide reduction, organic transformation reactions, and seawater uranium extraction. For different application scenarios, catalysts with suitable band structures were selected to meet the thermodynamic conditions required for catalytic reactions. Further structural regulation of the COFs can dynamically accelerate catalytic reactions, significantly enhancing the overall photocatalytic efficiency.[57]

3.2.1 Designing donor-acceptor structures

The extended π-conjugated framework in sp^2c-COFs provided a high-speed pathway for carrier separation and migration. The incorporation of electron-rich and electron-deficient units into the structure creates a periodic D-A system. This architecture enhances the electron push-pull effect, facilitates the migration of photogenerated charge carriers, and effectively suppresses the recombination of electron-hole pairs, thereby significantly improving the photocatalytic performance. Building blocks with appropriate electronegativity differences were selected, and suitable D-A systems were designed using strategies such as topological design, lattice capping, pore modification, and interlayer stacking (Fig. 3a). Precise control of the electron push-pull effects and band structures at the molecular level enables efficient separation and transport of photogenerated carriers in various application scenarios.[42,62,64,65]

The most commonly employed design strategy involves the selection of two building blocks with different electronegativities to form a two-component in-plane D-A system. As shown in Fig. 3(b), the thiophene unit, which acts as an electron donor, undergoes a Knoevenagel reaction with the electron-withdrawing thiazole unit, yielding cyano-substituted BTH-3 under the catalysis of $AcONH_4$. By modulating the electronic properties of aldehyde monomers, researchers discovered that the strong D-A effect within the COF framework effectively promoted intramolecular charge transfer (ICT) and suppressed carrier recombination, leading to a significant improvement in the catalytic hydrogen production performance.[66] Building on this foundation, a three-component in-plane D-π-A system can be developed further. Taking Fig. 3(c) as an example, by employing thiophene and triazine units as electron donors and acceptors, respectively, with PDAN serving as the linker, the resulting three-component COF-JLU35 exhibited outstanding planar π-conjugation properties and exceptional carrier separation efficiency. The three-component system exhibited more tunable band structures and optoelectronic properties, not only expanding the structural complexity of the framework but also providing new avenues for the precise design of novel sp^2c-COFs photocatalysts.[67] Furthermore, intramolecular D-A-D systems can be constructed through the design and synthesis of the monomers. Dong *et al*. synthesized a two-component DABT-Py-COF using a novel D-A-D monomer, DABT-4CHO, which contained quinoline (electron donor) and thiadiazole (electron acceptor) (Fig. 3d). Compared to conventional D-A COFs, the incorporation of D-A-D monomers enhances visible-light absorption while significantly promoting the ICT effect. This facilitates carrier separation and migration, resulting in photocatalytic COF materials with outstanding performance and long-term stability.[68]

Constructing D-A structures on the in-plane skeleton of COFs necessitates modifying their nodes or linkers, which inevitably alters the lattice structure. However, by utilizing unreacted functional groups at the lattice edges to introduce suitable donor-acceptor units, significant D-A effects can be induced at the electronic level, without changing the lattice structure.[42] Our research group integrated electron-donating thiophene units into the periphery of electron-withdrawing COF-TNOB lattices, yielding end-capped COF-TNOB-Ps (Fig. 3e). The end-capping modification forms a built-in heterojunction that promotes electron-hole pair separation, endowing COF-TNOB-Ps with enhanced light absorption capacity and photoresponse characteristics. This approach offers novel insights for designing and regulating the carrier separation properties in sp^2c-COFs.[49] Jiang *et al*. introduced electron-withdrawing fullerene units into the pores of electron-donating Zn-porphyrin frameworks *via* click chemistry, yielding $[C60]_y$-ZnPc-COFs with exceptional photocatalytic potential (Fig. 3f). The carrier concentration and charge separation efficiency can be precisely regulated by adjusting the fullerene content. The pore modification strategy leverages pore confinement effects and crystalline order, extending the types of donor and acceptor units from planar molecules to zero-dimensional molecular species, thereby further enriching structural design strategies for COFs.[69]

Beyond D-A systems connected *via* covalent bonds, supramolecular interactions offer an alternative pathway for developing interlayer D-A architectures. As illustrated in Fig. 3(g), Lin *et al*. constructed the first intercalated COF using electron-deficient, bulky perylene diimide units and electron-rich perylene molecules. Owing to the extensive π-surface overlap and buffering effect of planar perylene, steric hindrance was significantly reduced, enhancing the stability of columnar alternating stacking in the *z*-direction. The resulting intercalated COF exhibited markedly enhanced crystallini-

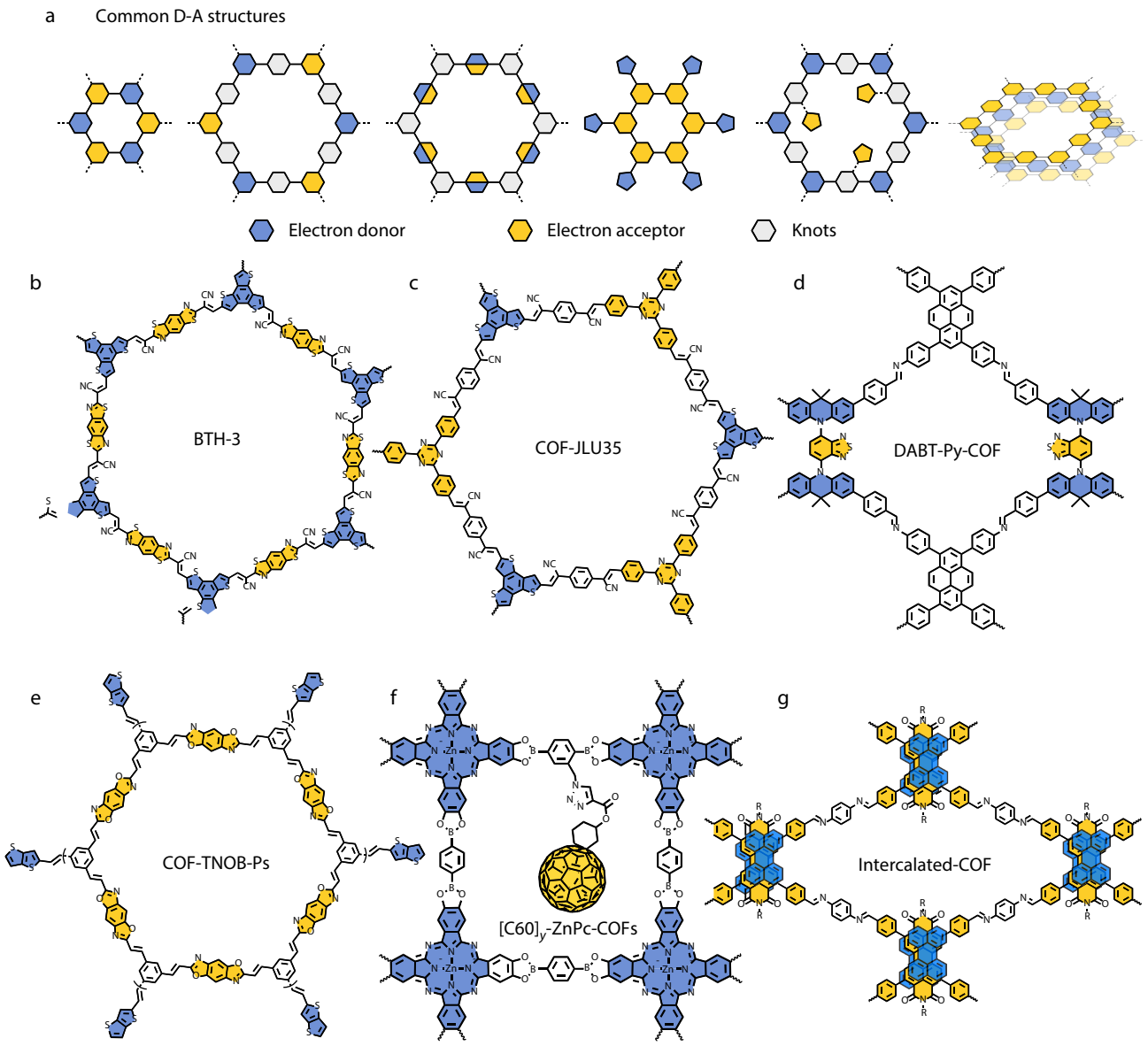

Fig. 3 (a) Common D-A structure design strategies; Schematics of (b) BTH-3, (c) COF-JLU35, (d) DABT-Py-COF, (e) COF-TNOB-Ps, (f) $[C60]_y$-ZnPc-COFs, and (g) Intercalated-COF.

ty and holds great promise for optoelectronic applications compared to its non-intercalated COF. This unique intercalation strategy enables the bottom-up construction of D-A systems in the *z*-direction, thereby opening new avenues for constructing diverse heterostructures.[70]

3.2.2 Crafting charged environments

Without altering the lattice structure of the COF framework, the introduction of charged functional groups can effectively modulate COFs' electronic structure and substrate affinity of COFs, enabling precise design of photocatalytic performance.[71,72] Common strategies include protonation modification and the use of zwitterionic building blocks.

Protonation modifications are typically applied at the N-site. Through immersion or steam treatment with acidic solutions such as ascorbic acid, sulfuric acid, hydrochloric acid, and phosphoric acid,[73–75] weak electrostatic interactions form between N and H, causing N to transform into $N\text{-}H^+$, thereby achieving protonic modification of N-containing monomers or skeletons in a single step.[76] Protonated COFs often exhibit unique optoelectronic properties and carrier mobility: N^+ redistributes framework charges, leading to non-uniform charge density. This not only enhances the planar conjugation of COFs, exposing more active sites, but also improves carrier separation efficiency.[77,78] Acid treatment of different intensities and concentrations can lead to varying degrees of acid chromism, significantly redshifting the light absorption range and shortening the band gap, thereby enhancing the overall light energy utilization efficiency.[72,76] Additionally, protonation enhances the hydrophilicity of COFs, facilitating the mass transfer of water molecules to active sites and improving substrate affinity for certain catalytic reactions. Therefore, protonation can simultaneously improve the

https://doi.org/10.1007/s10118-025-3550-0

photoelectric properties of COFs in terms of thermodynamics and kinetics, making them more suitable for photocatalytic applications.

As shown in Fig. 4(a), the protonation of the nitrogen atoms on the bipyridine units yielded TP-BPyN PCOF, which exhibited a substantially enhanced photocatalytic hydrogen evolution rate. Compared with the unmodified TP-BPyN COF, the hydrogen evolution rate increased from 6.457 mmol·g^{-1}·h^{-1} to 22.438 mmol·g^{-1}·h^{-1} (Fig. 4b). Protonation alters the charge density distribution, effectively reducing the exciton binding energy and promoting the generation of free charge. Simultaneously, the reduction in structural distortion significantly enhances the D-A effect and structural planarity of COFs, facilitating the transport of photogenerated carriers and thereby improving the hydrogen production activity in multiple aspects.[79] Wang *et al.* found that protonated COFs exhibit significantly enhanced interfacial hydrophilicity, which reduces particle aggregation in water, maximizes the exposure of active sites, and facilitates water access to the active sites within the pores.[81] In sp^{2}c-COFs, the protonated N$^+$ sites possess a stronger electron-withdrawing capability, thereby promoting charge carrier separation and transfer. Furthermore, protonation enhances the photostability of the skeleton and extends its visible-light absorption capability,[72] providing practical guidance for the construction of highly efficient and stable photocatalytic systems.

The protonated weak electrostatic interactions formed between N and H result in low stability and readily fail in basic environments. Furthermore, some COF structures do not incorporate N atoms, which significantly limits the application scope and structural design flexibility of the COF-based catalysts. Therefore, in certain scenarios where protonation modification is unsuitable, employing covalently bonded zwitterionic building blocks to synthesize zwitterionic carbon-organic frameworks (ZCOFs) featuring a pair of oppositely charged groups offers significant advantages. When these oppositely

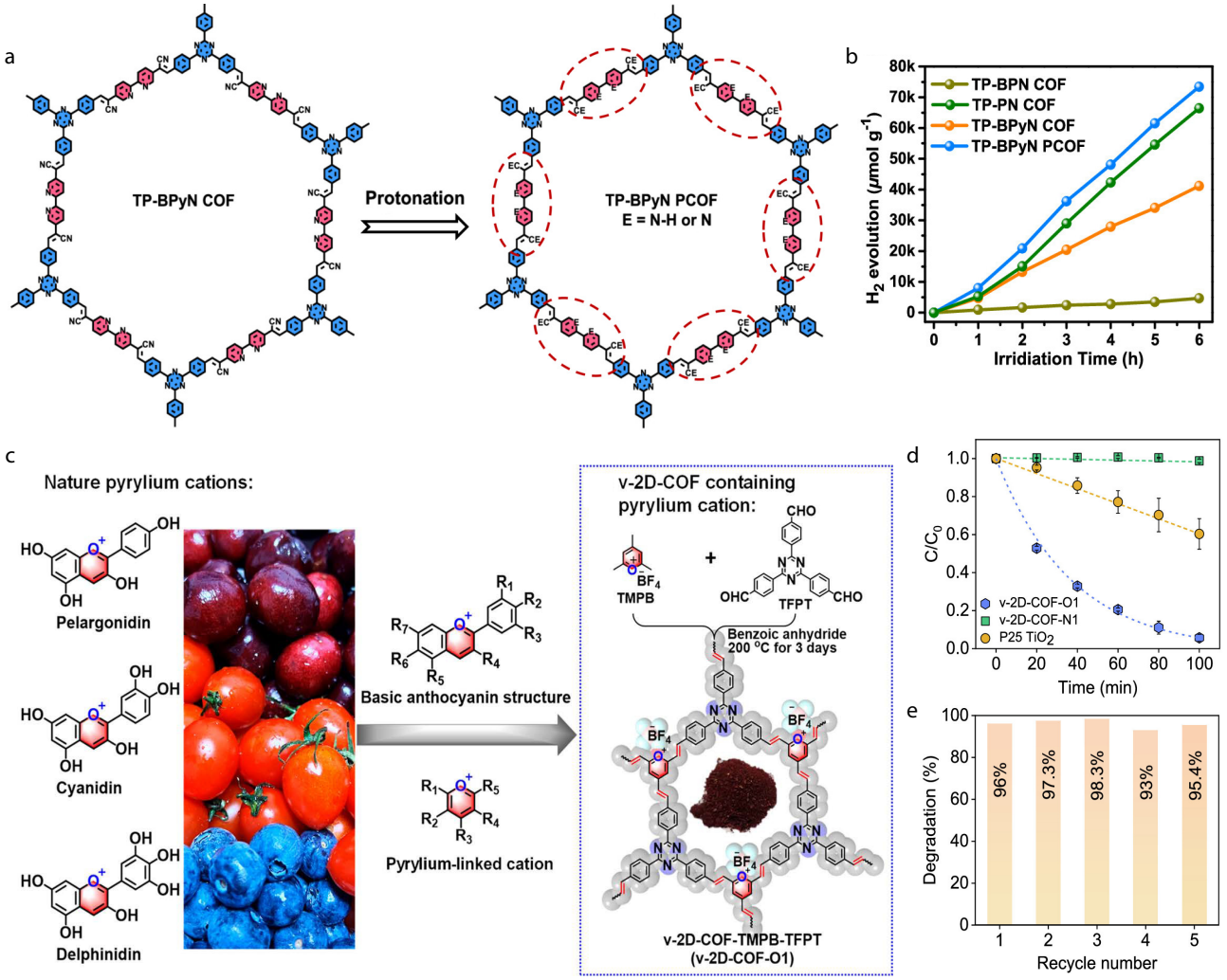

Fig. 4 (a) Schematic diagram of the protonation process of TP-BPyN COF (Reproduced with permission from Ref. [79]; Copyright (2024), American Chemical Society); (b) Photocatalytic hydrogen production activity of COFs loaded with 12 wt% Pt (Reproduced with permission from Ref. [79]; Copyright (2024), American Chemical Society); (c) Synthesis method of v-2D-COF-O1 inspired by anthocyanins in nature; (d, e) Photodegradation of methyl qrange and performance retention rate over five cycles; (c–e: reproduced with permission from Ref. [80]; Copyright (2023), American Chemical Society).

https://doi.org/10.1007/s10118-025-3550-0

charged building blocks are uniformly distributed at the molecular level, ZCOFs exhibit overall electrical neutrality. Owing to ionic solvation, the material exhibits strong hydration properties, which facilitate substrate adsorption and mass transfer during certain catalytic reactions.[82] The introduction of zwitterionic building blocks alters the charge distribution of the backbone, facilitating the generation, separation, and migration of the photogenerated charge carriers.

However, electrostatic repulsion between cations and anions affects the interlayer ordered stacking of ZCOFs, leading to amorphous or low-crystalline structures. Thus, the currently mature synthetic routes for ZCOFs are relatively few and revolve around three core strategies: post-synthetic modification for attaching ionic side chains,[83] one-pot protocol employing zwitterionic monomers,[80,84,85] and bottom-up methodology that incorporates specific functional monomers such as squaric acid.[86–88]

Pyran cations are six-membered heterocyclic systems that contain O^+ ions. Anthocyanins are key components of the natural pigment anthocyanin and play a vital role in photosynthesis and plant coloration. Inspired by this, we synthesized a v-2D-COF containing a pyran cationic group *via* a one-pot method (Fig. 4c). During photodegradation, photo-generated electrons migrate to oxygen to form reactive oxygen species (ROS) such as $\cdot O_2^-$. These ROS further react with water to generate additional ROS, ultimately leading to degradation of organic pollutants. Owing to the presence of zwitterionic monomers, v-2D-COFs efficiently activated oxygen molecules to generate highly oxidative ROS, exhibiting outstanding photocatalytic degradation activity and cycling stability in wastewater containing methyl orange (Figs. 4d and 4e), significantly outperforming v-2D-COF-N1 containing only pyran groups.[80]

Zhang *et al*. designed and synthesized a methyl monomer, 3-TPPS, featuring a sulfonate side-chain. This compound reacted with 1,3,5-tris(4-formylphenyl) triazine (TFPT) to produce Zi-VCOF-1, which exhibited outstanding hydrogen production performance (13.547 $mmol \cdot g^{-1} \cdot h^{-1}$). The introduction of the sulfonate side chain enhanced the hydrophilicity of the pore channels, thereby increasing the number of potential photocatalytic sites. Within the sulfonate-pyridinium zwitterion pair, the electron density at the maximum valence band and minimum conduction band are distributed near the sulfonate group and pyridine ring, respectively. This facilitated the rapid migration and separation of photogenerated carriers along the "sulfonate-pyridine ring-COF skeleton" pathway.[84] Xu *et al*. developed a green hydrothermal method for the synthesis of Zi-VCOF-1. Benefiting from its suitable band structure, highly ordered conjugated plane, and abundant hydrophilic side chains, the Zi-VCOF-1 membrane device subsequently demonstrated outstanding hydrogen production performance of 402.1 $mmol \cdot h^{-1} \cdot m^{-2}$.[85]

Employing a functional squaric acid monomer as a building block is another strategy for creating ZCOFs. The spatial isolation of the monomer mitigates electrostatic repulsions, allowing the formation of a locally charge-polarized yet highly ordered layered framework. This synergistically enhances bulk charge separation and visible-light harvesting capability, leading to superior catalytic performance.[87,88] This study provides a viable strategy for the design and functional integration of ZCOFs.

3.2.3 Constructing COFs-based heterojunctions

Combining two or more different materials to form a heterojunction not only preserves the inherent advantages of each component, but also addresses issues such as insufficient activity and processing difficulties in single semiconductors. Therefore, constructing heterojunctions is an effective approach for enhancing the carrier utilization efficiency of COF-based photocatalysts.[56,89–91] Common types of heterojunctions include II-scheme, Z-scheme, and S-scheme, with distinct carrier transport mechanisms in each heterojunction.

In the II-scheme heterojunctions, both the VB and CB of semiconductor 1 (S1) were higher than those of semiconductor 2 (S2). Upon exposure to visible light, electrons and holes accumulate in the CB of S2 and VB of S1, respectively, achieving effective separation of the photogenerated carriers.[56] As shown in Fig. 5(a), the cyano group adsorbs onto TiO_2 *via* strong interfacial coordination bonds and undergoes *in situ* polymerization with aldehyde monomers on the TiO_2 surface, forming a COF-TiO_2 heterojunction with a dense interface. Because both the VB and CB of TiO_2 are higher than those of COF, under light irradiation, photogenerated electrons migrate directionally from COF to TiO_2 along the N-Ti covalent bond, forming a typical organic-inorganic II-scheme heterojunction. The N-Ti covalent bond significantly enhances the interfacial charge transfer and prevents electron-hole pair recombination. Concurrently, the II-scheme heterojunction exhibited extended light-absorption capabilities and demonstrated outstanding photocatalytic uranium reduction activity, achieving a U^{VI} removal rate as high as 99.8% within 40 min. The *in situ* bridging strategy provides a convenient and efficient method for heterojunction preparation and expands the scope of photocatalytic applications.[92]

To address the issue of weaker redox capability in II-scheme heterojunctions, holes in the VB of S1 recombine with electrons in the CB of S2 in Z-scheme heterojunctions. The remaining electrons and holes then accumulate at the CB of S1 and the VB of S2, respectively, achieving electron-hole pair separation through a different mechanism. Owing to the accumulation of electrons at the negative energy level and holes at the positive energy level, the Z-scheme heterojunction exhibits enhanced redox capabilities, effectively boosting the catalytic efficiency of COF-based photocatalysts.[95] The Lan group designed and synthesized a COF-semiconductor Z-type heterojunction for artificial photosynthesis (Fig. 5b). A series of COF-oxide semiconductor heterojunctions (CoF-SC: COF-TiO_2, Bi_2WO_6 and α-Fe_2O_3) were obtained by covalent bonding with polyarylether COFs through hydroxyl functional groups on the surface of the oxide semiconductors. In this heterojunction, photogenerated electrons accumulated on the COF are utilized for CO_2 reduction, whereas the holes generated in the oxide semiconductor are consumed for water oxidation. The presence of pyridine and cyano groups within the COF lowered the energy barrier for CO_2 reduction. Moreover, the effective covalent coupling between the organic framework and semiconductor enables highly efficient transfer of photogenerated charge carriers across the interface. This synergistic design ultimately leads

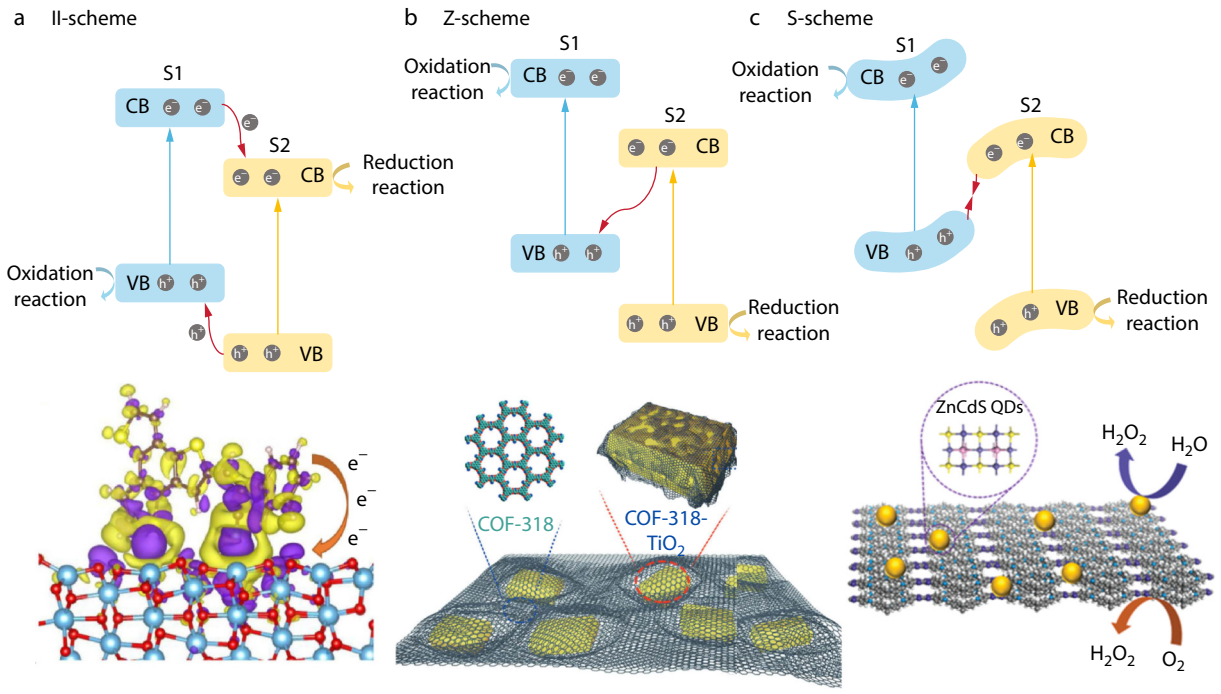

Fig. 5 (a) Schematic diagram of the II-scheme heterojunctions band structure and covalently bonded COF-TiO_2 (Reproduced with permission from Ref. [92]; Copyright (2024), Elsevier B.V.); (b) Schematic diagram of the Z-scheme heterojunctions band structure and COF-318-SCs (Reproduced with permission from Ref. [93]; Copyright (2020), Wiley-VCH Verlag GmbH & Co. KGaA, Weinheim); (c) Schematic diagram of the S-scheme heterojunctions band structure and TT-COF/ZCS (Reproduced with permission from Ref. [94]; Copyright (2024), Wiley-VCH GmbH).

to the direct construction of an efficient artificial photosynthesis system.[93]

The S-scheme heterojunction differs in that the energy bands of S1 and S2 bend upward and downward, respectively, and within the built-in electric field they point from S1 to S2. Under the drive of an electric field, the electrons in the CB of S2 recombine with the holes in the VB of S1. Therefore, S1 and S2 are positively and negatively charged, respectively, undergoing oxidation and reduction reactions (Fig. 5c).[96] To address the issues of low redox efficiency and easy recombination of photogenerated carriers in COFs, Jiang *et al*. uniformly anchored zero-dimensional quantum dots onto the surface of a two-dimensional TT-COF, resulting in an S-scheme heterojunction TT-COF/ZCS with enhanced photocatalytic production efficiency for H_2O_2. The formation of the S-scheme heterojunction effectively prevented ZCS agglomeration while modulating the band structure of the TT-COF, significantly enhancing the overall photogenerated carrier mobility and redox capability. TT-COF/ZCS achieved an outstanding H_2O_2 production rate of 5171 $\mu mol \cdot g^{-1} \cdot h^{-1}$, far surpassing the catalytic performances of TT-COF and ZCS alone. S-type heterojunctions predominantly exhibit outstanding redox capabilities, providing a highly promising platform for the coupled design of COF-based photocatalysts.

3.2.4 Modifying COFs pores

Crystalline COFs featuring periodic frameworks and extended π-conjugated structures have tremendous potential for application in photocatalysis. Chou *et al*. discovered that regulating the solvent polarity can enhance the crystallinity of COFs. Owing to their long-range ordered crystal structures, highly crystalline samples exhibit superior carrier migration pathways and demonstrate outstanding hydrogen production performance.[97] The long-range order characteristics of crystalline materials promote carrier separation and reduce charge trapping at the defect sites.

However, the layered stacking structure of COFs tends to slip in water, leading to a severe disruption or even disorder in the crystal lattice. During photocatalytic processes, inevitable corrosion and degradation lead to the distortion and deformation of the main chain. Weak interlayer interactions then induce distortion and deformation in the other layers, limiting the planar π-conjugated expansion within the crystal framework. Because the conjugated length of COFs affects the migration of photogenerated carriers, structural distortion may affect the photocatalytic performance, limiting the application scenarios and long-term service stability of COF-based catalysts.[98] Therefore, selecting an appropriate pore modification strategy to maintain the ordered stacking of COFs during the catalytic process can promote intralayer carrier migration and even enable interlayer hopping. Simultaneously, the well-ordered stacked pores also facilitate the transport of reactants, enhancing the overall catalytic efficiency.

To mitigate the adverse effects of structural distortions, Guo *et al*. employed a unique polymer pore-filling strategy to suppress the detrimental impact of interlayer dislocations. As a functional object, polyethylene glycol (PEG) penetrates the one-dimensional channels of BT-COF *via* low-pressure driving after high-temperature melting, forming the PEG@BT-COF composite (Fig. 6a). Owing to the dense packing of poly-

mer chains, interlayer misalignment can be effectively suppressed by extending the PEG segments, thereby maintaining ordered coaxial stacking. Therefore, ordered stacking of PEG@BT-COF was maintained during the photocatalytic process. Enhanced interlayer π-stacking promotes interlayer carrier transport and prolongs exciton lifetime, significantly boosting the photocatalytic hydrogen production performance and cyclic structural stability.[99] This pore-filling strategy is also applicable to various two-dimensional COFs, demonstrating considerable universality.

Although polymer pore filling can maintain the ordered interlayer structure of COFs, hydrocarbon chain polymers are highly disordered and lack conjugation, making it impossible to further improve the electronic conductivity of COFs. Based on this, Vaidhyanathan *et al*. adopted a post-modification strategy to covalently link pyrrole molecules into COFs channels and cross-link them to form conductive one-dimensional poly pyrrole chains, obtaining a quasi-three-dimensional framework (Fig. 6b). Owing to the presence of out-of-plane conductive "conjugated bridges," poorly conductive two-dimensional COFs are transformed into conductive quasi-three-dimensional COFs, featuring reduced bandgaps and additional conductive pathways. This topological transformation delivers distinct bonding advantages, not only enhancing the stability and porosity of COFs, but also improving the electronic conductivity.[100] The Lan research group directly employed thiophene-containing aldehyde monomers and a one-step polymerization strategy to synthesize COF-PTh grafted with polythiophene chains, thereby minimizing the impact of post-modification steps on COFs' crystallinity and functional group purity of COFs. Under visible-light irradiation, COF-PTh rapidly generates superoxide radicals ($O_2^{\bullet-}$), which efficiently drive the synthesis of 4(3H)-quinazolinone *via* dehydrogenative cross-coupling with high conversion and selectivity. The spatial confinement of the thiophene unit and the conductive advantage of the polythiophene chain synergistically optimize the interlayer charge transport and structural stability without compromising crystallographic perfection, establishing a versatile and precisely tunable design strategy for three-dimensional frameworks.[102]

Beyond the strategy of introducing specific polymeric components, the direct utilization of the monomers' intrinsic bonding motifs enables in-plane to 3D structural conversion through *z*-directional cross-linking. As shown in Fig. 6(c), the imine bonds in the 2D imine COF (Py-BDA-COF) undergo a sulfidation reaction to form conjugated and stable thiazole rings, whereas the diyne units (—C≡C—C≡C—) undergo thermal polymerization and cross-linking along the *z*-axis, forming "conjugated pillars" (—C≡C—C=C—) with an alternating "alkyne-alkene" arrangement. The resulting 3D-Py-BDA-S-COF exhibits complete conjugation in all three dimensionsin the plane (*x*, *y*) and interlayer (*z*) directions, combin-

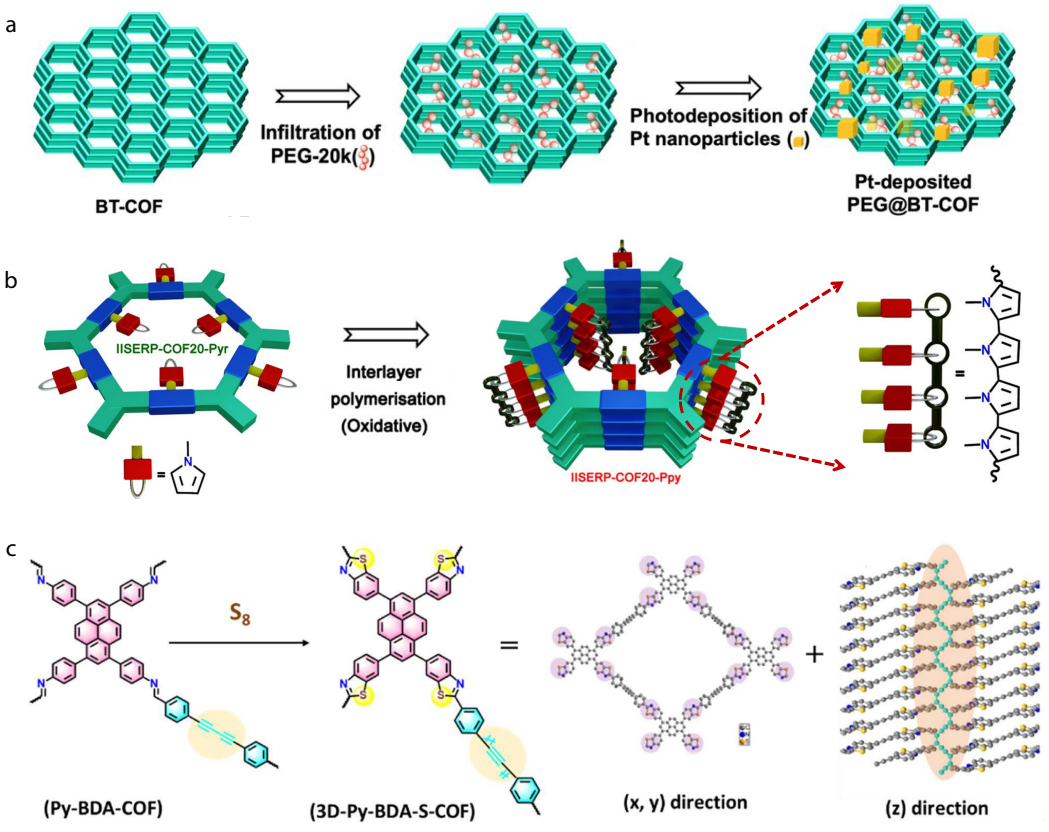

Fig. 6 (a) Schematic diagram of the preparation of PEG@BT-COF filled with polyethylene glycol (Reproduced with permission from Ref. [99]; Copyright (2021), The Authors); (b) Schematic diagram of the preparation of IISERP-COF20-Ppy with polypyrrole interlayer knitting (Reproduced with permission from Ref. [100]; Copyright (2024), American Chemical Society); (c) Schematic diagram of the preparation of (z)-crosslinked 3D-Py-BDA-S-COF (Reproduced with permission from Ref. [101]; Copyright (2025), American Chemical Society).

ing the essential properties of highly efficient photocatalysts: 3D π-conjugation, high crystallinity, and high porosity. Additionally, the sulfur atom on the thiazole ring possesses a lone pair of electrons, acting as an electron donor to generate a donor-acceptor (D-A) effect, which significantly enhances the degree of electron delocalization in COFs. This approach achieves three-dimensional delocalization of π electrons while preserving the integrity of the skeletal structure, thereby significantly enhancing the electronic properties of the material and demonstrating outstanding performance in the photocatalytic reduction of nitrobenzene.[101]

4 APPLICATIONS OF SP^{2}C-COFS IN THE FIELD OF PHOTOCATALYSIS

Sp^{2}c-COFs possess a unique porous structure, outstanding physicochemical stability, exceptional charge-carrier separation efficiency, and flexible structural designability, making them a highly promising photocatalyst design platform with broad development prospects.[29,103–106] Next, we summarize and discuss the practical applications of sp^{2}c-COFs-based photocatalysts in water splitting hydrogen production, hydrogen peroxide production, carbon dioxide reduction, organic transformation reactions, and uranium extraction from seawater.[64,107–114]

4.1 Photocatalytic Hydrogen Production

To address the growing energy crisis and environmental pollution, developing photocatalytic water splitting technology by harnessing abundant solar energy is crucial for achieving green hydrogen generation and advancing the transformation of our energy landscape.[3,4,6] COFs possess unique inherent advantages, boasting substantial research foundations and promising technological prospects in the field of photocatalytic hydrogen production.

In 2014, the Lotsch group synthesized hydrazine-linked TF-PT-COFs using TFPT and 2,5-diethoxyphthalimide (DETH). Employing Pt as a cocatalyst, they achieved the first photocatalytic hydrogen production using a COF-based catalyst.[115] The photocatalytic hydrogen production mechanism of COFs materials is shown in Fig. 7(a). Most COFs require the assistance of co-catalysts such as Pt and electron sacrificial agents (ascorbic acid, triethanolamine, *etc*.) during the catalytic process to achieve rapid charge carrier separation and highly efficient redox reactions. Over the past few decades, researchers have focused on sp^{2}c-COFs that exhibit superior stability and conjugation and have explored strategies to enhance photocatalytic performance through multiple approaches, including structural design of materials and regulation of catalytic systems.

To address the difficulties in synthesizing and the scarcity of sp^{2}c-COFs, our research group has proposed a distinctive azole-induced aldol polycondensation strategy. The electron-deficient thiazole, oxazole, and thiadiazole groups activate the connected methyl groups, thereby mediating the aldol condensation reaction. This approach efficiently constructed multiple highly crystalline sp^{2}c-COFs with outstanding optoelectronic activities. We synthesized two isomeric benzobisoxazole aldehyde monomers, which were reacted with trimethylbenzene formaldehyde (BTCA) to yield two v-2D-COFs exhibiting different optoelectronic properties. Among these, v-2D-COF-NO1 containing trans-oxazole building blocks exhibited an outstanding light absorption capacity and charge carrier mobility (Fig. 7b). With Pt as the co-catalyst, v-2D-COF-NO1 exhibited a photocatalytic hydrogen production rate of 1.97 mmol·h^{-1}·g^{-1}, significantly outperforming the v-2D-COF-NO2 with the same framework (0.86 mmol·h^{-1}·g^{-1}). We believe that v-2D-COF-NO1 exhibits enhanced electron transfer processes, featuring a higher photoelectron migration efficiency from its active sites to Pt nanoparticles, thereby contributing to improved photocatalytic hydrogen production activity.[40] This study employed an oxazole-mediated aldol condensation strategy to synthesize two sp^{2}c-COFs with distinct photocatalytic properties, providing insights for the design and synthesis of isomerous semiconductor COFs materials.

Subsequently, we further extended the universality of the azole-induced aldol condensation strategy by reacting benzobis(thiazole) monomers with BTCA to synthesize v-2D-COF-NS1, which exhibited an enhanced hydrogen production performance (Fig. 7c). The electron-deficient thiazole unit and planar π-conjugated structure endow v-2D-COF-NS1 with a strong carrier separation capability and a narrow bandgap (1.85 eV), enabling it to exhibit a photocatalytic hydrogen production performance of 4.4 mmol·h^{-1}·g^{-1}. In highly ordered two-dimensional frameworks, light-induced exciton dissociation is more pronounced than in linear polymers of the same composition, thereby endowing sp^{2}c-COFs with superior hydrogen production capabilities.[48]

Building on this foundation, we further achieved a thiadiazole-mediated aldol condensation reaction, yielding sp^{2}c-COF-ST with outstanding physicochemical stability and optoelectronic response properties (Figs. 7d and 7e). To further validate the influence of the linker structure on the photocatalytic hydrogen production performance, we also synthesized partially imine-linked mix-COF-SNTs and fully imine-linked imi-COF-SNNTs. Despite sharing similar structural units, temperature-dependent photoluminescence (PL) measurements and density functional theory (DFT) calculations revealed that sp^{2}c-COF-ST with C=C exhibited smaller exciton binding energies and effective electron masses. This facilitates exciton dissociation and photogenerated carrier migration, thereby significantly enhancing the photocatalytic activity.[50] This series of studies demonstrates the feasibility and scalability of an azole-induced aldol condensation strategy, pioneering a novel approach for the design and synthesis of sp^{2}c-COFs photocatalysts.

4.2 Photocatalytic Hydrogen Peroxide Production

Hydrogen peroxide (H_2O_2) is a highly valuable green oxidizing agent with extensive applications in multiple fields, including wastewater treatment, healthcare, and energy storage.[108,116–119] However, traditional anthraquinone preparation methods suffer from drawbacks such as high cost and environmental pollution. Therefore, the selection of suitable photocatalysts for the synthesis of H_2O_2 using water and oxygen *via* the two-electron oxygen reduction pathway ($2e^-$ ORR: $O_2 + 2e^- + 2H^+ \rightarrow H_2O_2$) represents an eco-friendly green alternative.

Previous studies have demonstrated that cyano groups in sp^{2}c-COFs can promote the reduction of O_2 to H_2O_2. However, cyano-functionalized sp^{2}c-COFs (CN-COFs) still suffer from

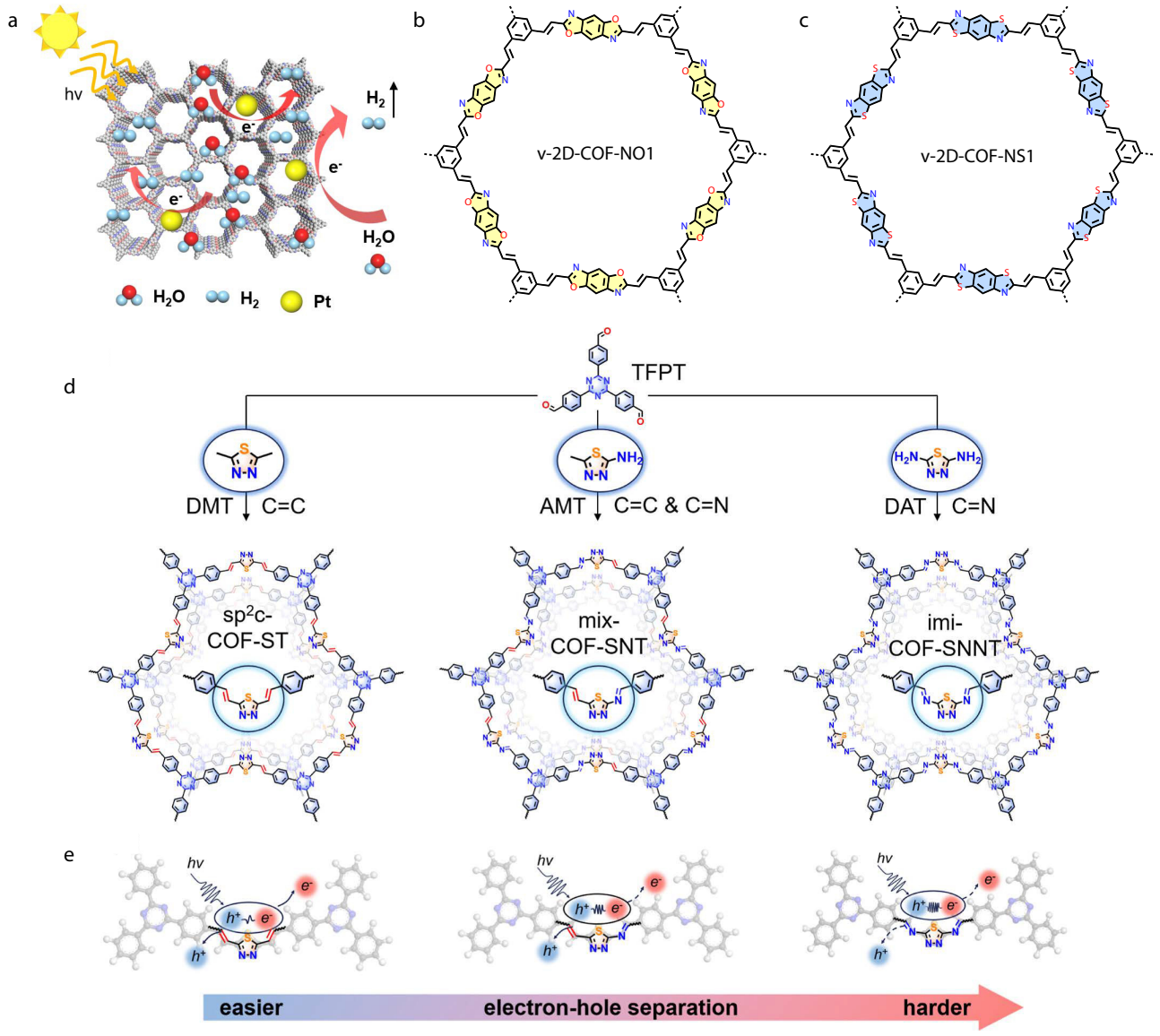

Fig. 7 (a) Schematic diagram of photocatalytic hydrogen production using COFs materials (Reproduced with permission from Ref. [49]; Copyright (2023), Elsevier Ltd.); (b, c) Schematic diagram of structures v-2D-COF-NO1 and v-2D-COF-NS1; (d, e) Synthetic routes and photoexcited carrier separation ability of sp^2c-COF-ST, mix-COF-SNT, and imi-COF-SNNT (Reproduced with permission from Ref. [50]; Copyright (2024), American Chemical Society).

limitations such as restricted oxygen capture capacity, insufficient charge separation, and rapid carrier recombination, which collectively constrain their overall performance in photocatalytic H_2O_2 production.[120–122] To address this issue, Hua *et al*. introduced amidoxime (AO) groups into sp^2c-COFs *via* cyanohydrination (Fig. 8a). PTTN-AO exhibited an exceptionally high H_2O_2 generation rate of 6024 $\mu mol \cdot h^{-1} \cdot g^{-1}$. The introduction of the AO group not only enhanced the hydrophilicity of the COF but also stabilized oxygen adsorption through hydrogen bonding, significantly improving the substrate affinity of the catalyst. Furthermore, it optimizes the charge distribution within the framework, promoting the separation and migration of photogenerated carriers, thereby facilitating photocatalytic reactions involving oxygen reduction and water oxidation.[123] Fig. 8(b) illustrates a potential catalytic mechanism for PTTN-AO: oxygen adsorbs onto the AO site and reacts with charge carriers *via* two distinct ORR pathways to generate H_2O_2. Holes and water undergo a four-electron WOR process to produce O_2, thereby sustaining the catalytic cycle.[124]

As shown in Fig. 8(c), BBT-ACN COF-1 with a typical D-A structure was constructed using the thiazole and thiophene groups. Compared to the π-A structure BBT-CAN COF-2, BBT-ACN COF-1 exhibits a lower exciton binding energy and a threefold higher photocatalytic H_2O_2 production efficiency, fully validating the effectiveness and universality of the D-A strategy in the field of photocatalysis.[125]

Utilizing a methyl-diazapyrene monomer, in which the methyl groups were activated by electron-withdrawing N atoms, the Zhang group constructed polycyclic aromatic hydrocarbon COFs (PAH-COFs) *via* Knoevenagel condensation with trimethylolpropane (Figs. 8d and 8e). The pyridine ring

not only enhances the backbone polarity of sp²c-COFs, improving the charge separation efficiency and hydrophilicity, but also serves as an active site to boost the photocatalytic reaction efficiency. Furthermore, the polycyclic aromatic hydrocarbon building block provides extended π-conjugation and significant semiconductor properties for the COFs. Consequently, g-COF-DMDP-1 exhibits outstanding photocatalytic activity and stability under visible light, demonstrating a hydrogen peroxide generation rate as high as 17080 $\mu mol \cdot h^{-1} \cdot g^{-1}$ in the presence of a hole sacrificial agent (Fig. 8f).[126]

4.3 Photocatalytic Carbon Dioxide Reduction

The excessive extraction and combustion of fossil fuels have led to massive CO_2 emissions, causing severe greenhouse effects and energy crises. Therefore, developing suitable photocatalyt-

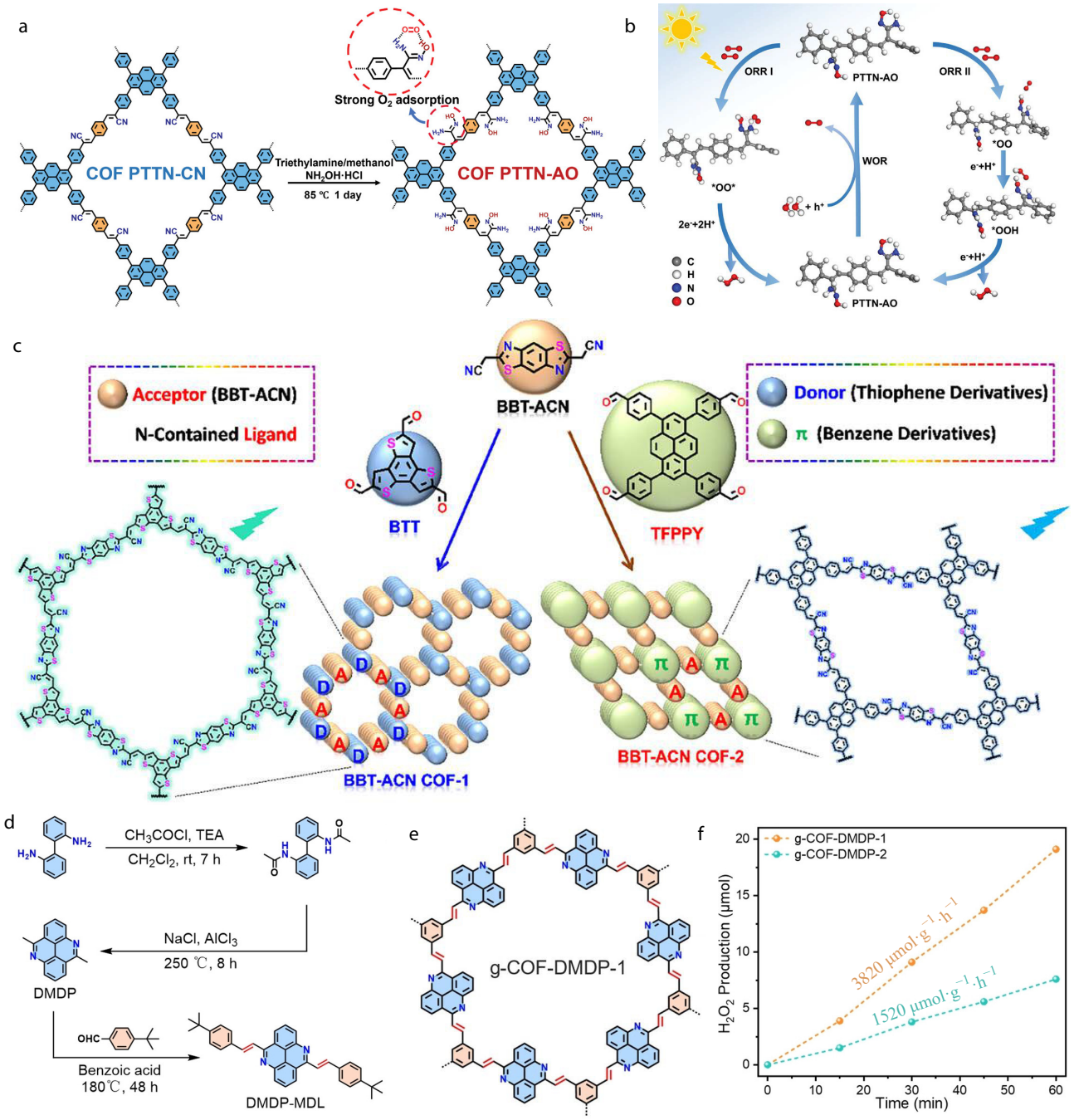

Fig. 8 (a) Synthesis of PTTN-AO; (b) Proposed reaction mechanism toward H_2O_2 production on the PTTN-AO; (a, b: reproduced with permission from Ref. [124]; Copyright (2025), The Author(s). Advanced Science published by Wiley-VCH GmbH). (c) Schematic representation for the construction of BBT- ACN COFs (Reproduced with permission from Ref. [125]; Copyright (2025), Wiley-VCH GmbH); (d) Synthesis of the key monomer DMDP and model compound DMDP-MDL; (e) g-COF-DMDP-1; (f) Time profiles of H_2O_2 production for g-COF-DMDP-1 and g-COF-DMDP-2; (d–f: reproduced with permission from Ref. [126]; Copyright (2024), Wiley-VCH GmbH).

https://doi.org/10.1007/s10118-025-3550-0

ic systems to convert excess CO_2 into other high-value-added products (such as CO, CH_4, and HCOOH) can not only achieve carbon neutrality goals, but also effectively alleviate energy shortages.[127–131]

Sp^2c-COFs possess regular lattice pores and layered stacking, making them highly amenable to the formation of heterostructures with other two-dimensional materials. Among them, graphene oxide (GO) has an efficient carrier transfer capacity and can be combined with COFs to construct heterojunction composite materials, solving the problems of the high carrier recombination rate and limited light absorption range of a single catalyst. As shown in Fig. 9(a), an S-scheme heterojunction was constructed *via* electrostatic self-assembly, leveraging the strong interactions between TP-COF and PRGO. The curved band structure enables the effective separation of electron-hole pairs, ensuring sufficient electrons for CO_2 reduction to CO. With infrared thermal energy assistance, the photothermal effect generated by PRGO suppressed carrier recombination. Adjusting the PRGO content can change the photoelectron-generation efficiency of the heterojunction (Fig. 9b). The heterojunction of 25% PRGO/TP-COF exhibited optimal synergistic effects, demonstrating an excellent CO yield and stability (Fig. 9c).[132]

Photogenerated electrons can participate in the reduction half-reaction of CO_2, whereas photogenerated holes can simultaneously engage in the oxidation half-reaction. Therefore, developing an efficient photocatalytic system that simultaneously utilizes both photogenerated electrons and holes to carry out the two half-reactions could significantly enhance carrier utilization and the overall economic value of the photocatalytic reaction. As shown in Fig. 9(d), Han *et al*. obtained viCOF-bpy-Re through $Re(CO)_5Cl$ treatment, which exhibited both CO generation performance (190.6 $\mu mol \cdot g^{-1} \cdot h^{-1}$ with approximately 100% selectivity) and O_2 generation performance (90.2 $\mu mol \cdot g^{-1} \cdot h^{-1}$). The low-polarity π-conjugation between the Re-complex and triazine ring enhances the charge separation capability of viCOF-bpy-Re, enabling the simultaneous participation of electron-hole pairs in CO_2 reduction and H_2O oxidation through intramolecular charge transfer processes. Compared to isolated COF and $Re(CO)_5Cl$, viCOF-bpy-Re exhibits outstanding catalytic performance and long-term stability, providing a paradigm for designing complex coupled photocatalytic systems.[133]

4.4 Photocatalytic Organic Conversion Reactions

The use of photocatalysis for organic transformations is a sustainable and eco-friendly strategy for synthesizing fine chemicals because it significantly reduces economic costs and minimizes the formation of hazardous by-products. Owing to their unique strengths, sp^2c-COFs are gaining considerable momentum in this area and have already exhibited remarkable catalytic performances across diverse reaction types (Fig. 10a).[134–143]

Zhang *et al*. synthesized ionic sp^2c-COFs (ivCOF-O) using methyl-substituted pyran cationic monomers under organic proton-acid catalysis. Subsequently, ammonia gas was employed as a nucleophile to replace O – with N *in situ*, yielding a neutral pyridine-based vCOF-N. Owing to the differences in

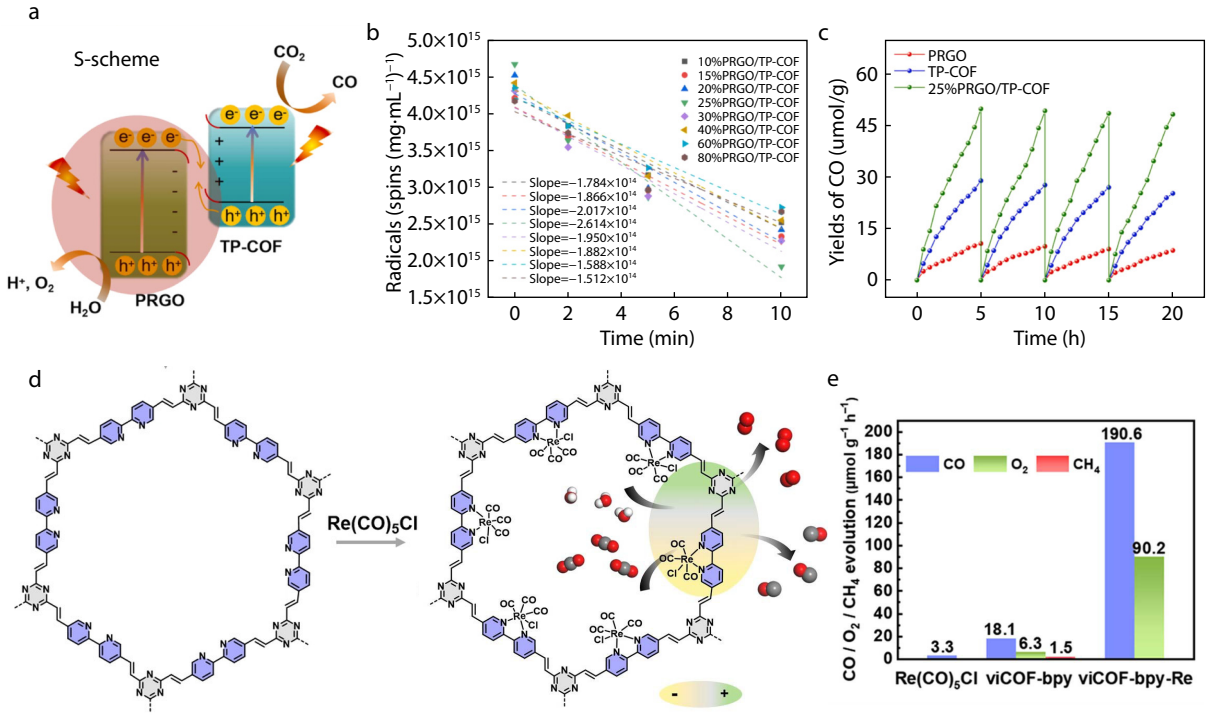

Fig. 9 (a) Potential mechanism of CO_2 Reduction and band structure of 25% PRGO/TP-COF; (b) Linear fitting of ESR signals to visible light irradiation time of TEMPO in *X*% PRGO/TP-COF samples; (c) Comparison of photocatalytic cycle performance of TP-COF, PRGO and 25% PRGO/TP-COF; (a–c: reproduced with permission from Ref. [132]; Copyright (2024), Elsevier B.V.). (d) Synthesis methods and catalytic mechanism of viCOF-bpy-Re; (e) Photocatalytic CO_2 reduction performance of Re-complex, viCOF-bpy, and viCOF-bpy-Re; (d, e: reproduced with permission from Ref. [133]; Copyright (2023), Wiley-VCH GmbH).

the heteroatoms, these two sp²c-COFs exhibit distinct charge states and band structures despite sharing identical electronic structures. Based on their respective semiconductor characteristics, ivCOF-O exhibited high activity in [2+2+2] cycloaddition reactions, whereas vCOF-N effectively catalyzed the coupling reaction between aryl ketones and benzylamines (Fig. 10b). This study demonstrates a precisely tunable heteroatom-embedding approach and a design strategy for highly efficient photocatalysts for organic transformations.[144]

Fig. 10(c) shows a special heteroporous structure. Two sp²c-COFs (g-TPYP-COF and g-TPYBP-COF) with the D-π-A effect were successfully constructed by the reaction of the hexacofunctional C_3 methyl monomer with the C_2 aldehyde

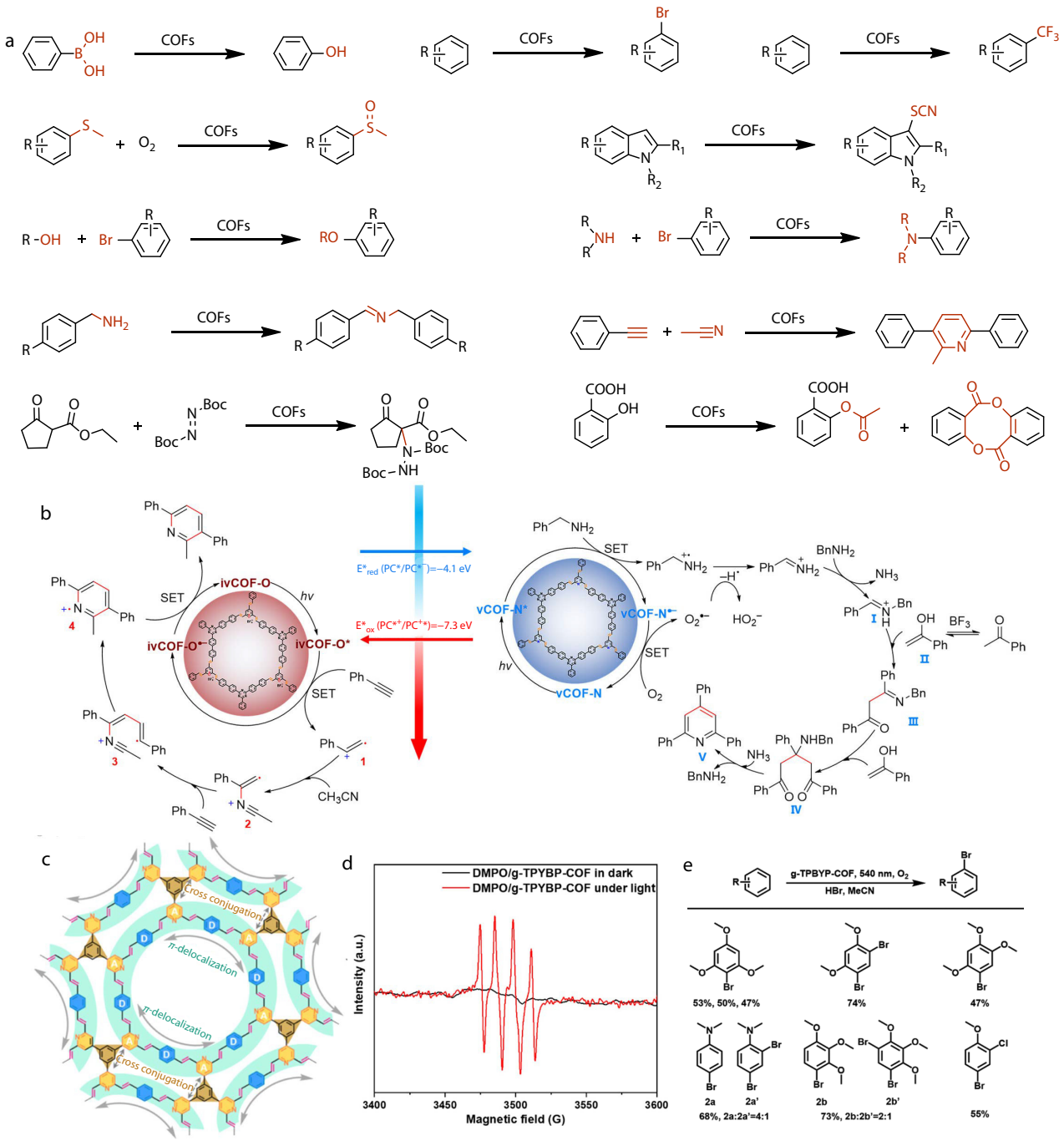

Fig. 10 (a) Organic transformation reactions catalyzed by sp²c-COFs; (b) Plausible mechanism for the photocatalytic reactions catalyzed by ivCOF-O and vCOF-N (Reproduced with permission from Ref. [144]; Copyright (2021), Wiley-VCH GmbH); (c) Schematic Diagram of D-π-A Alignment within the in-Plane Skeleton of g-TPYBP-COF; (d) EPR spectra of DMPO-$O2^{-}$ using g-TPYBP-COF as a photocatalyst; (e) Substrate Scope for the Photocatalytic Bromination of Arenes; (c–e: Reproduced with permission from Ref. [145]; Copyright (2023), American Chemical Society).

https://doi.org/10.1007/s10118-025-3550-0

monomer. An extended π-dispersed structural unit is formed around the double-layered hexagonal channel. Electron paramagnetic resonance (EPR) analysis indicated that, under green light irradiation, both COFs efficiently generated ROS ($O_2^{\bullet-}$) *via* singlet electron transfer and produced $^1O_2$ through triplet electron exchange (Fig. 10d). Therefore, when HBr served as the bromine source and oxygen as the clean oxidant, g-TPYBP-COF efficiently achieved the photocatalytic bromination of aromatic or thiophene derivatives. g-TPYBP-COF exhibited conversion rates and regioselectivity based on pore size distribution, along with excellent cycling stability (Fig. 10e).[145]

4.5 Photocatalytic Uranium Extraction

The nuclear power industry holds a significant position in the current energy system owing to its numerous advantages, including high energy density, low carbon emissions, and environmental friendliness. Among these, uranium (U), as the primary fuel for nuclear power, is crucial for the sustainable development of nuclear energy as a primary fuel for nuclear power. Given the limited terrestrial uranium reserves, obtaining uranium from seawater through environmentally friendly photocatalytic methods represents a promising strategy.[123,146–148] Owing to their stable framework, high specific surface area, and readily tunable pore structure, sp^2c-COFs have demonstrated remarkable selectivity, high adsorption capacity, and fast kinetics in photocatalytic uranium extraction from seawater, garnering significant research interest.

The real marine environment is extremely complex and is characterized by severe marine biofouling contamination, high concentrations of competing metal ions, and extremely low uranium concentrations, all of which affect the long-term high-efficiency operation of catalysts.

Qiu *et al.* designed a sp^2c-COF with both anti-biological contamination activity and a high uranium extraction capacity, named PT-BN-AO (Fig. 11a). The triazine unit endows PT-BN-AO with outstanding semiconductor properties and highly planar π-conjugated structures in the crystalline state, significantly enhancing the separation and migration of the photogenerated carriers. Under visible-light irradiation, the triazine unit generates ROS with biotoxicity, enabling resistance against complex marine bacteria. Concurrently, redox

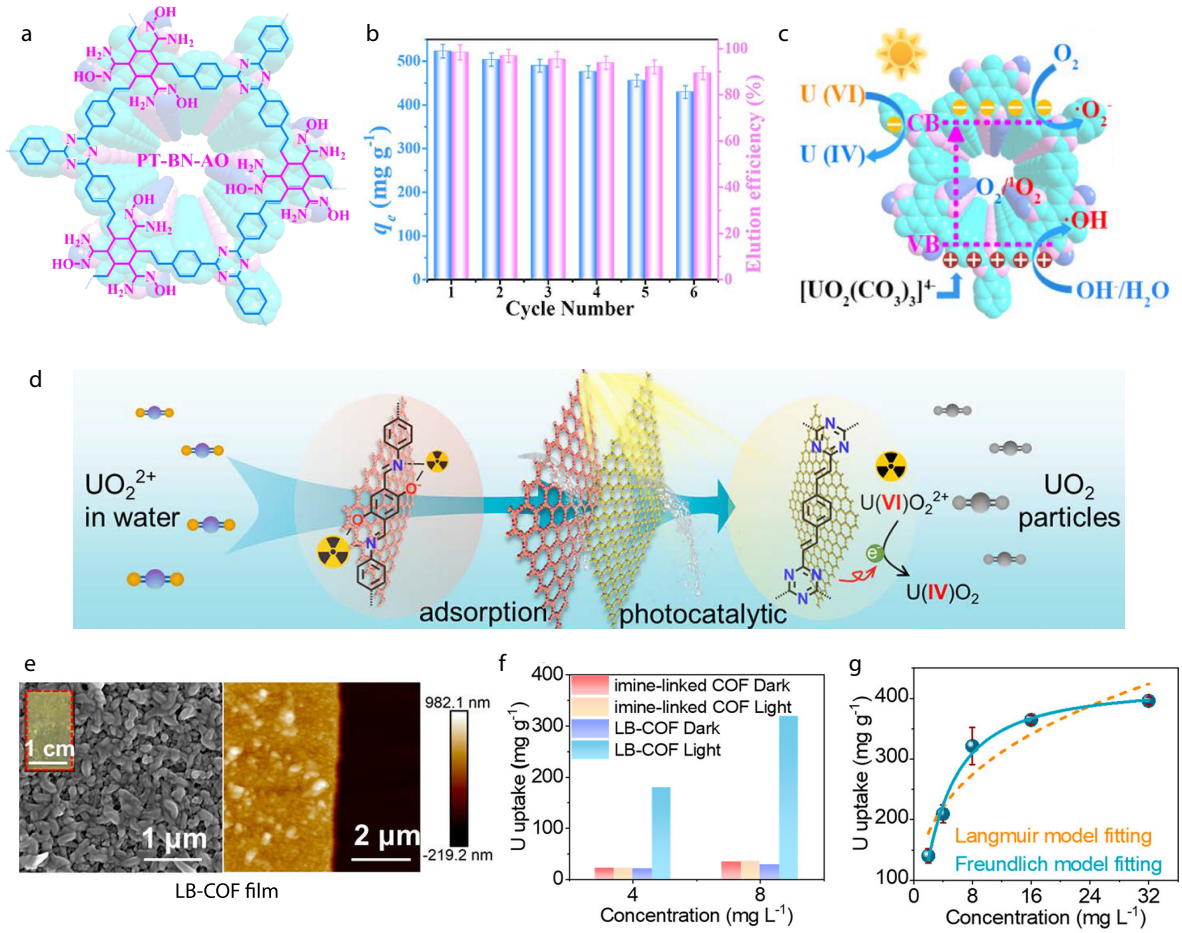

Fig. 11 (a) PT-BN-AO; (b) Reusability and elution efficiency of PT-BN-AO for extracting uranium; (c) Mechanism of photoenhanced extraction of uranium by PT-BN-AO; (a–c: reproduced with permission from Ref. [149]; Copyright (2021), American Chemical Society). (d) Schematic diagram of photocatalytic UO_2^{2+} reduction; (e) AFM images of imine-linked COF and LB-COF films; (f) Uranium extraction capacity of COF films under light and dark conditions; (g) Equilibrium adsorption isotherms of LB-film and the corresponding fitting curves based on Langmuir model and Freundlich model under simulated sunlight irradiation; (d–g: reproduced with permission from Ref. [150], Copyright (2024), American Chemical Society).

reactions at the interface reduce U^{VI} to insoluble U^{IV}, demonstrating a uranium extraction performance of 5.78 mg·g^{-1} without sacrificial agents (Figs. 11b and 11c).[149]

Inspired by block copolymers (BCPs),[151] we prepared a layer-blocked COF (LB-COF) heterogeneous film *via* surface-initiated Schiff base condensation and aldol condensation (Fig. 11d). First, we grew a uniform imine COF film on the surface of an aminated Si wafer. By utilizing the unreacted aldehyde groups at the edges to initiate aldol condensation, we grew a layer of sp^{2}c-COFs. LB-COF films combine the high crystallinity of imine COFs with the outstanding optoelectronic activity of sp^{2}c-COFs. Their photocatalytic uranium extraction capacity (320 mg·g^{-1}) significantly exceeded that of standalone imine COFs (35 mg·g^{-1}) and sp^{2}c-COFs (295 mg·g^{-1}) (Figs. 11f and 11g). XPS and theoretical calculations revealed that the electron-withdrawing N atoms in triazine serve as active sites for electron transfer. Photogenerated electrons are transferred from LB-COF to uranyl ions and N atoms within the triazine structure, enabling the efficient reduction and extraction of uranium.[150]

5 SUMMARY AND OUTLOOK

In conclusion, this review summarizes recent research progress on sp^{2}c-COFs in the field of photocatalysis, covering their structural design and synthesis, strategies for enhancing photocatalytic performance, and application studies. First, we provide a comprehensive overview of the design principles and synthetic methodologies of sp^{2}c-COFs. Reactions such as the Knoevenagel condensation and aldol condensation enable the construction of sp^{2}c-COFs with diverse topological structures. We subsequently summarize strategies for enhancing the photocatalytic performance of sp^{2}c-COFs, guided by mechanistic insights and application requirements. These include designing D-A structures, building charged environments, developing heterojunctions, and employing polymer hole-transport scaffolds. Finally, we elaborate on the applications of sp^{2}c-COF-based photocatalysts in fields such as H_2 production, H_2O_2 production, CO_2 reduction, organic transformation reactions, and uranium extraction from seawater.

Although sp^{2}c-COFs have demonstrated excellent development prospects for various photocatalytic reactions in recent years, the practical application of sp^{2}c-COF materials in photocatalytic engineering is still in its infancy. However, numerous challenges remain to be addressed.

(1) Currently, most sp^{2}c-COFs require reactions under harsh high-temperature and high-pressure conditions, consuming large amounts of organic solvents during both the synthesis and washing processes. This significantly increases the economic costs and environmental pressures. Therefore, exploring and developing green, efficient, and large-scale synthesis methods is crucial for advancing the practical application of sp^{2}c-COFs-based photocatalysts.

(2) Although sp^{2}c-COFs-based materials have demonstrated remarkable photocatalytic performance in laboratory settings, investigations of their stability and efficacy under real-world application conditions remain limited. Therefore, to advance these materials from laboratory research to practical deployment, it is imperative to address the diverse challenges in real-world environments through rational structural design that enhances their crystallinity, stability, and overall durability.

(3) Certain catalytic systems require the addition of sacrificial agents to achieve efficient oxidation/reduction half-reactions, which not only increases costs but also leads to the wastage of photogenerated carriers. Therefore, by leveraging the intrinsic structural design of sp^{2}c-COFs or constructing heterojunctions, oxidation and reduction half-reactions can be simultaneously realized. This approach enhances the utilization efficiency of light energy while increasing the added value of catalytic reactions.

(4) The widespread use of sp^{2}c-COF photocatalysts is currently limited by their powder morphology, which leads to processing and recyclability issues. To overcome these engineering barriers, the development of macroscopic structures such as membranes and gels designed for specific operational environments is pivotal for transitioning these materials from the laboratory to practical applications.

BIOGRAPHY

Tao Zhang received his B.S. degree in chemistry from Sichuan University in 2008, and his Ph.D. degree from Dresden University of Technology in 2015. Currently, he is a researcher at the Ningbo Institute of Materials Technology & Engineering, Chinese Academy of Sciences, and the head of the research group of interface functional polymer materials. His main research interests include 2D conjugated/porous polymers, polymer films and coatings, photocatalysis energy conversion, and organic semiconductor devices.

Conflict of Interests

The authors declare no interest conflict.

ACKNOWLEDGMENTS

This work was financially supported by the Ningbo "3315 Innovation Programme" (No. 2019-17-C), the National Natural Science Fund for Excellent Young Scholars (No. 52322316), the Intergovernmental International Science and Technology Innovation Cooperation of the National Key R&D Program of China (No. 2025YFE0151500), the Distinguished Youth Foundation of Zhejiang Provincial Natural Science Foundation of China (No. LRG25E030001), China Postdoctoral Science Foundation (No. 2024M753340), and Zhejiang Provincial Natural Science Foundation of China (No. LQN25B040004), and the Ningbo Natural Science Foundation (No. 2024J115).

REFERENCES

1 Ren, J.; Zhao, D. Recent advances in reticular chemistry for clean energy, global warming, and water shortage solutions. *Adv. Funct. Mater.* **2023**, *34*, 2307778.
2 Boettcher, S.W. Introduction to green hydrogen. *Chem. Rev.* **2024**, *124*, 13095−13098.
3 Lv, J.; Xie, J.; Mohamed, A.G.A.; Zhang, X.; Feng, Y.; Jiao, L.; Zhou, E.; Yuan, D.; Wang, Y. Solar utilization beyond photosynthesis.

Graphical Abstract

Design, Synthesis, and Photocatalytic Applications of sp^2-Carbon-Conjugated Organic Frameworks

Meng-Yao Chen, Guang-En Fu, Wen-Kai Zhao, and Tao Zhang

Ningbo Institute of Materials Technology & Engineering, Chinese Academy of Sciences; University of Chinese Academy of Science; Zhejiang University

This work reviews recent advances in sp^2-carbon-conjugated organic frameworks with ethylene-bonded linkers for photocatalysis, outlines the design principles and synthesis methods of sp^2c-COFs and systematically summarizes various strategies for enhancing photocatalytic performance, and finally discusses challenges and future prospects for sp^2c-COFs in practical photocatalytic applications.

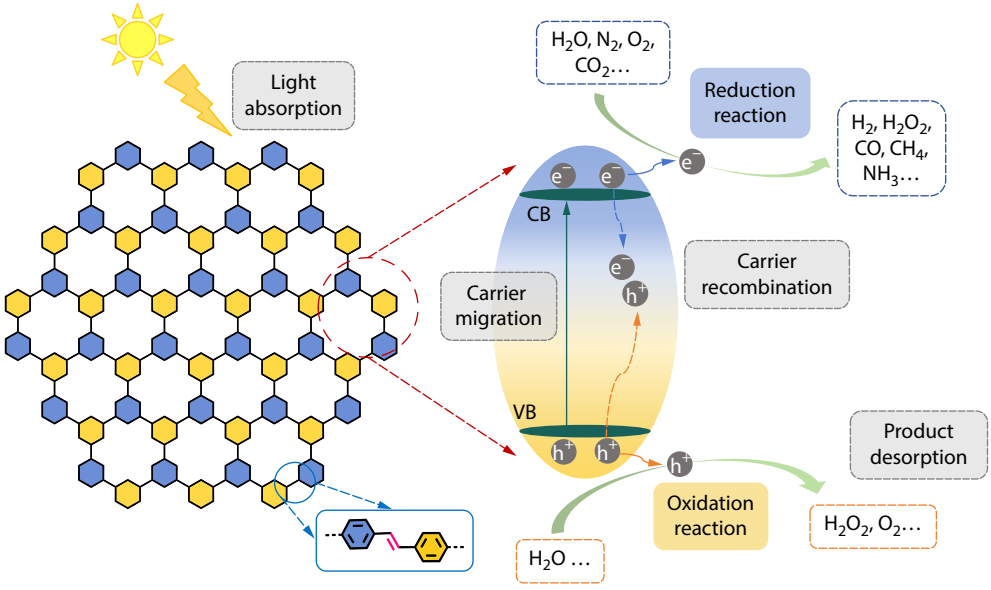

Chinese J. Polym. Sci., 2026 *https://doi.org/10.1007/s10118-025-3550-0*

Nat. Rev. Chem. **2022**, *7*, 91–105.
4 Zhou, L.; Li, X.; Ni, G.W.; Zhu, S.; Zhu, J. The revival of thermal utilization from the sun: interfacial solar vapor generation. *Natl. Sci. Rev.* **2019**, *6*, 562–578.
5 Romero, E.; Novoderezhkin, V.I.; Van Grondelle, R. Quantum design of photosynthesis for bio-inspired solar-energy conversion. *Nature* **2017**, *543*, 355–365.
6 Lewis, N.S. Research opportunities to advance solar energy utilization. *Science* **2016**, *351*, aad1920.
7 Zhang, X.-L.; Wang, L.; Chen, L.; Ma, X.-Y.; Xu, H.-X. Ultrathin 2D conjugated polymer nanosheets for solar fuel generation. *Chinese J. Polym. Sci.* **2019**, *37*, 101–114.
8 Hu, X.-L.; Li, H.-G.; Tan, B.-E. COFs-based porous materials for photocatalytic applications. *Chinese J. Polym. Sci.* **2020**, *38*, 673–684.
9 Fujishima, A.; Honda, K. Electrochemical photolysis of water at a semiconductor electrode. *Nature* **1972**, *238*, 37–38.
10 Nishiyama, H.; Yamada, T.; Nakabayashi, M.; Maehara, Y.; Yamaguchi, M.; Kuromiya, Y.; Nagatsuma, Y.; Tokudome, H.; Akiyama, S.; Watanabe, T.; Narushima, R.; Okunaka, S.; Shibata, N.; Takata, T.; Hisatomi, T.; Domen, K. Photocatalytic solar hydrogen production from water on a 100-m^2 scale. *Nature* **2021**, *598*, 304–307.
11 Weller, T.; Sann, J.; Marschall, R. Pore structure controlling the activity of mesoporous crystalline $CsTaWO_6$ for photocatalytic hydrogen generation. *Adv. Energy Mater.* **2016**, *6*, 1600208.
12 Sun, B.; Zhou, W.; Li, H.; Ren, L.; Qiao, P.; Li, W.; Fu, H. Synthesis of particulate hierarchical tandem heterojunctions toward optimized photocatalytic hydrogen production. *Adv. Mater.* **2018**, *30*, 1804282.
13 Hou, H.; Zeng, X.; Zhang, X. Production of hydrogen peroxide by photocatalytic processes. *Angew. Chem. Int. Ed.* **2020**, *59*, 17356–17376.
14 Karamoschos, N.; Tasis, D. Photocatalytic evolution of hydrogen peroxide: a minireview. *Energies* **2022**, *15*, 6202.
15 Wu, Q.; Cao, J.; Wang, X.; Liu, Y.; Zhao, Y.; Wang, H.; Liu, Y.; Huang, H.; Liao, F.; Shao, M.; Kang, Z. A metal-free photocatalyst for highly efficient hydrogen peroxide photoproduction in real seawater. *Nat. Commun.* **2021**, *12*, 483.
16 Liu, B.; Qian, Z.; Shi, X.; Su, H.; Zhang, W.; Kludze, A.; Zheng, Y.; He, C.; Yanagi, R.; Hu, S. Solar-driven selective conversion of millimolar dissolved carbon to fuels with molecular flux

generation. *Nat. Commun.* **2025**, *16*, 1558.
17 Zhang, Y.; Guan, X.; Meng, Z.; Jiang, H. L. Supramolecularly built local electric field microenvironment around cobalt phthalocyanine in covalent organic frameworks for enhanced photocatalysis. *J. Am. Chem. Soc.* **2025**, *147*, 3776–3785.
18 Lu, W.; Tait, C.E.; Avci, G.; Li, X.; Crumpton, A.E.; Shao, P.; Aitchison, C.M.; Ceugniet, F.; Yao, Y.; Frogley, M.D.; Decarolis, D.; Yao, N.; Jelfs, K.E.; McCulloch, I. Cobalt-embedded metal–covalent organic frameworks for CO_2 photoreduction. *J. Am. Chem. Soc.* **2025**, *147*, 9056–9061.
19 Li, H.; Yang, Y.; He, C.; Zeng, L.; Duan, C. Mixed-ligand metal–organic framework for two-photon responsive photocatalytic C–N and C–C coupling reactions. *ACS Catal.* **2019**, *9*, 422–430.
20 Zadehnazari, A.; Khosropour, A.; Altaf, A.A.; Rosen, A.S.; Abbaspourrad, A. Tetrazine-linked covalent organic frameworks with acid sensing and photocatalytic activity. *Adv. Mater.* **2024**, *36*, 2311042.
21 Zhang, P.; Wang, Z.; Wang, S.; Wang, J.; Liu, J.; Wang, T.; Chen, Y.; Cheng, P.; Zhang, Z. Fabricating industry-compatible olefin-linked COF resins for oxoanion pollutant scavenging. *Angew. Chem. Int. Ed.* **2022**, *61*, e202213247.
22 Papailias, I.; Todorova, N.; Giannakopoulou, T.; Ioannidis, N.; Dallas, P.; Dimotikali, D.; Trapalis, C. Novel torus shaped g-C_3N_4 photocatalysts. *App. Catal. B: Environ.* **2020**, *268*, 118733.
23 Bao, T.; Li, X.; Li, S.; Rao, H.; Men, X.; She, P.; Qin, J. Recent advances of graphitic carbon nitride (g-C_3N_4) based materials for photocatalytic applications: a review. *Nano Mater. Sci.* **2025**, *7*, 145–168.
24 Cheng, L.; Xiang, Q.; Liao, Y.; Zhang, H. CdS-based photocatalysts. *Energy Environ. Sci.* **2018**, *11*, 1362–1391.
25 Sun, Q.; Wang, N.; Yu, J.; Yu, J.C. A hollow porous CdS photocatalyst. *Adv. Mater.* **2018**, *30*, 1804368.
26 Guo, Q.; Zhou, C.; Ma, Z.; Yang, X. Fundamentals of TiO_2 Photocatalysis: concepts, mechanisms, and challenges. *Adv. Mater.* **2019**, *31*, 1901997.
27 Guo, Q.; Ma, Z.; Zhou, C.; Ren, Z.; Yang, X. Single molecule photocatalysis on TiO_2 surfaces: focus review. *Chem. Rev.* **2019**, *119*, 11020–11041.
28 Huang, N.; Wang, P.; Jiang, D. Covalent organic frameworks: a materials platform for structural and functional designs. *Nat. Rev. Mater.* **2016**, *1*, 16068.
29 Xu, S.; Richter, M.; Feng, X. Vinylene-linked two-dimensional covalent organic frameworks: synthesis and functions. *Acc. Mater. Res.* **2021**, *2*, 252–265.
30 Lyu, H.; Diercks, C.S.; Zhu, C.; Yaghi, O.M. Porous crystalline olefin-linked covalent organic frameworks. *J. Am. Chem. Soc.* **2019**, *141*, 6848–6852.
31 Diercks, C.S.; Yaghi, O.M. The atom, the molecule, and the covalent organic framework. *Science* **2017**, *355*, eaal1585.
32 Liu, Y.; Zhou, W.; Teo, W.L.; Wang, K.; Zhang, L.; Zeng, Y.; Zhao, Y. Covalent-organic-framework-based composite materials. *Chem* **2020**, *6*, 3172–3202.
33 Zhao, W. K.; Li, S. X.; Fu, G. E.; Zhang, T. Structural design, controlled preparation and applications of two-dimensional sp2c-conjugated polymers. *Acta Polymerica Sinica* (in Chinese), **2024**, *55*, 532–552.
34 Zhang, Y.; Lv, W.; Wang, F.; Niu, X.; Wang, G.; Wu, X.; Zhang, X.; Chen, X. Room temperature in-situ preparation of hydrazine-linked covalent organic frameworks coated capillaries for separation and determination of polycyclic aromatic hydrocarbons. *Front. Chem. Sci. Eng.* **2023**, *17*, 548–556.
35 Li, T.; Xiong, J.; Chen, M.; Shi, Q.; Li, X.; Jiang, Y.; Feng, Y.; Zhang, B. A tunable ionic covalent organic framework platform for efficient CO_2 catalytic conversion. *Front. Chem. Sci. Eng.* **2024**, *18*, 3.
36 Zhuang, X.; Zhao, W.; Zhang, F.; Cao, Y.; Liu, F.; Bi, S.; Feng, X. A two-dimensional conjugated polymer framework with fully sp^2-bonded carbon skeleton. *Polym. Chem.* **2016**, *7*, 4176–4181.
37 Yang, Q.; Chen, Y.; Liu, N.; Li, S.; Chen, M.; Zheng, W.; Fu, Y.; Han, J.; Rodriguez, R.D.; Hou, Y.; Zhang, T. Enhanced nanoconfinement of copper-organic interfaces within phthalocyanine frameworks for selective electroreduction of CO to acetate. *J. Am. Chem. Soc.* **2025**, *147*, 22132–22140.
38 Yang, H.; Han, J.; Li, S.; Petkov, P. St.; Xue, Q.; Feng, X.; Zhang, T. Synthesis of crystalline two-dimensional conjugated polymers through irreversible chemistry under mild conditions. *Nat. Commun.* **2025**, *16*, 2336.
39 Wang, K.; Yang, H.; Liao, Z.; Li, S.; Hambsch, M.; Fu, G.; Mannsfeld, S. C. B.; Sun, Q.; Zhang, T. Monolayer-assisted surface-initiated schiff-base-mediated aldol polycondensation for the synthesis of crystalline sp^2 carbon-conjugated covalent organic framework thin films. *J. Am. Chem. Soc.* **2023**, *145*, 5203–5210.
40 Li, S.; Xu, S.; Lin, E.; Wang, T.; Yang, H.; Han, J.; Zhao, Y.; Xue, Q.; Samorì, P.; Zhang, Z.; Zhang, T. Synthesis of single-crystalline sp^2-carbon-linked covalent organic frameworks through imine-to-olefin transformation. *Nat. Chem.* **2025**, *17*, 226–232.
41 Yan, H.; Kou, Z.; Li, S.; Zhang, T. Synthesis of sp^2 carbon-conjugated covalent organic framework thin-films via copper-surface-mediated knoevenagel polycondensation. *Small* **2023**, *19*, 2207972.
42 Jin, E.; Lan, Z.; Jiang, Q.; Geng, K.; Li, G.; Wang, X.; Jiang, D. 2D sp^2 carbon-conjugated covalent organic frameworks for photocatalytic hydrogen production from water. *Chem* **2019**, *5*, 1632–1647.
43 Jin, E.; Asada, M.; Xu, Q.; Dalapati, S.; Addicoat, M.A.; Brady, M.A.; Xu, H.; Nakamura, T.; Heine, T.; Chen, Q.; Jiang, D. Two-dimensional sp^2 carbon–conjugated covalent organic frameworks. *Science* **2017**, *357*, 673–676.
44 Sun, H.; Ji, H.; Qiao, D.; Xu, Y.; Qu, X.; Qi, Y.; Feng, Z.; Zhang, X.; Zhang, F.; Wang, R.; Dong, B. Vinylene-linked covalent organic frameworks based on phenanthroline for visible-light-driven bifunctional photocatalytic water splitting. *Chem. Eng. J.* **2025**, *507*, 160448.
45 Zheng, Z.; Rampal, N.; Inizan, T.J.; Borgs, C.; Chayes, J. T.; Yaghi, O. M. Large language models for reticular chemistry. *Nat. Rev. Mater.* **2025**, *10*, 369–381.
46 Lyu, H.; Ji, Z.; Wuttke, S.; Yaghi, O.M. Digital reticular chemistry. *Chem* **2020**, *6*, 2219–2241.
47 Becker, D.; Biswal, B. P.; Kaleńczuk, P.; Chandrasekhar, N.; Giebeler, L.; Addicoat, M.; Paasch, S.; Brunner, E.; Leo, K.; Dianat, A.; Cuniberti, G.; Berger, R.; Feng, X. Fully sp^2-carbon-linked crystalline two-dimensional conjugated polymers: insight into 2D poly(phenylenecyanovinylene) formation and its optoelectronic properties. *Chem. Eur. J.* **2019**, *25*, 6562–6568.
48 Li, S.; Ma, R.; Xu, S.; Zheng, T.; Wang, H.; Fu, G.; Yang, H.; Hou, Y.; Liao, Z.; Wu, B.; Feng, X.; Wu, L.; Li, X.; Zhang, T. Two-dimensional benzobisthiazole-vinylene-linked covalent organic frameworks outperform one-dimensional counterparts in photocatalysis. *ACS Catal.* **2023**, *13*, 1089–1096.
49 Fu, G.; Ma, R.; Xu, S.; Xu, T.; Li, S.; Zhao, Y.; Jing, Y.; Li, X.-B.; Zhang, T. Edge-engineering of donor-acceptor sp^2-carbon-conjugated covalent organic frameworks for high-performance photocatalysts. *Mater. Today Energy* **2024**, *40*, 101477.
50 Fu, G.; Yang, D.; Xu, S.; Li, S.; Zhao, Y.; Yang, H.; Wu, D.; Petkov, P.S.; Lan, Z. A.; Wang, X.; Zhang, T. Construction of thiadiazole-bridged sp^2-carbon-conjugated covalent organic frameworks with diminished excitation binding energy toward superior photocatalysis. *J. Am. Chem. Soc.* **2024**, *146*, 1318–132.

51 Pastoetter, D.L.; Xu, S.; Borrelli, M.; Addicoat, M.; Biswal, B.P.; Paasch, S.; Dianat, A.; Thomas, H.; Berger, R.; Reineke, S.; Brunner, E.; Cuniberti, G.; Richter, M.; Feng, X. Synthesis of vinylene-linked two-dimensional conjugated polymers via the horner–wadsworth–emmons reaction. *Angew. Chem. Int. Ed.* **2020**, *59*, 23620–23625.

52 Liu, Y.; Fu, S.; Pastoetter, D.L.; Khan, A.H.; Zhang, Y.; Dianat, A.; Xu, S.; Liao, Z.; Richter, M.; Yu, M.; Položij, M.; Brunner, E.; Cuniberti, G.; Heine, T.; Bonn, M.; Wang, H.; Feng, X. Vinylene-linked 2D conjugated covalent organic frameworks by wittig reactions. *Angew. Chem. Int. Ed.* **2022**, *61*, e202209762.

53 Sun, L.; Liang, Z.; Yu, J.; Xu, R. Luminescent microporous organic polymers containing the 1,3,5-tri(4-ethenylphenyl) benzene unit constructed by heck coupling reaction. *Polym. Chem.* **2013**, *4*, 1932–1938.

54 Niu, C. P.; Zhang C. R.; Liu, X.; Liang, R. P.; Qiu, J. D. Synthesis of propenone-linked covalent organic frameworks via Claisen-Schmidt reaction for photocatalytic removal of uranium. *Nat. Commun.* **2023**, *14*, 4420.

55 Baly, E.C.C.; Heilbron, I.M.; Barker, W.F. CX.—photocatalysis. part I. the synthesis of formaldehyde and carbohydrates from carbon dioxide and water. *J. Chem. Soc.* **1921**, *119*, 1025–1035.

56 Qi, S.; Guo, R.; Bi, Z.; Zhang, Z.; Li, C.; Pan, W. Recent progress of covalent organic frameworks-based materials in photocatalytic applications: a review. *Small* **2023**, *19*, 2303632.

57 Dong, H.; Qu, C.; Li, C.; Hu, B.; Li, X.; Liang, G.; Jiang, J. Recent advances of covalent organic frameworks-based photocatalysts: principles, designs, and applications. *Chin. J. Catal.* **2025**, *70*, 142–206.

58 Wang, Y.; Suzuki, H.; Xie, J.; Tomita, O.; Martin, D.J.; Higashi, M.; Kong, D.; Abe, R.; Tang, J. Mimicking natural photosynthesis: solar to renewable H_2 fuel synthesis by z-scheme water splitting systems. *Chem. Rev.* **2018**, *118*, 5201–5241.

59 Banerjee, T.; Podjaski, F.; Kröger, J.; Biswal, B.P.; Lotsch, B.V. Polymer photocatalysts for solar-to-chemical energy conversion. *Nat. Rev. Mater.* **2020**, *6*, 168–190.

60 Ghosh, S.; Nakada, A.; Springer, M.A.; Kawaguchi, T.; Suzuki, K.; Kaji, H.; Baburin, I.; Kuc, A.; Heine, T.; Suzuki, H.; Abe, R.; Seki, S. Identification of prime factors to maximize the photocatalytic hydrogen evolution of covalent organic frameworks. *J. Am. Chem. Soc*. **2020**, 9752–9762.

61 Zhang, T.; Chen, S.; Petkov, P. St.; Zhang, P.; Qi, H.; Nguyen, N.N.; Zhang, W.; Yoon, J.; Li, P.; Brumme, T.; Alfonsov, A.; Liao, Z.; Hambsch, M.; Xu, S.; Mester, L.; Kataev, V.; Büchner, B.; Mannsfeld, S.C.B.; Zschech, E.; Parkin, S.S.P.; Kaiser, U.; Heine, T.; Dong, R.; Hillenbrand, R.; Feng, X. Two-dimensional polyaniline crystal with metallic out-of-plane conductivity. *Nature* **2025**, *638*, 411–417.

62 Fu, G.; Yang, H.; Zhao, W.; Samorì, P.; Zhang, T. 2D conjugated polymer thin films for organic electronics: opportunities and challenges. *Adv. Mater*. **2024**, 2311541.

63 Chen, M.; Fu, G.; Zhao, W.; Zhang, T. Effective strategies in covalent organic frameworks for enhanced photocatalytic hydrogen production. *Chem. Eur. J.* **2025**, *31*, e202500100.

64 Shen, R.; Li, X.; Qin, C.; Zhang, P.; Li, X. Efficient photocatalytic hydrogen evolution by modulating excitonic effects in Ni-intercalated covalent organic frameworks. *Adv. Energy Mater.* **2023**, *13*, 2203695.

65 Wang, Y.; Qiao, Z.; Li, H.; Zhang, R.; Xiang, Z.; Cao, D.; Wang, S. Molecular engineering for modulating photocatalytic hydrogen evolution of fully conjugated 3D covalent organic frameworks. *Angew. Chem. Int. Ed.* **2024**, *63*, e202404726.

66 Wang, Y.; Hao, W.; Liu, H.; Chen, R.; Pan, Q.; Li, Z.; Zhao, Y. Facile construction of fully sp^2-carbon conjugated two-dimensional covalent organic frameworks containing benzobisthiazole units. *Nat. Commun.* **2022**, *13*, 100.

67 Li, Z.; Deng, T.; Ma, S.; Zhang, Z.; Wu, G.; Wang, J.; Li, Q.; Xia, H.; Yang, S.-W.; Liu, X. Three-component donor–π–acceptor covalent–organic frameworks for boosting photocatalytic hydrogen evolution. *J. Am. Chem. Soc.* **2023**, *145*, 8364–8374.

68 Wang, G.-B.; Xu, H.-P.; Xie, K.-H.; Kan, J.-L.; Fan, J.; Wang, Y.-J.; Geng, Y.; Dong, Y.-B. A covalent organic framework constructed from a donor–acceptor–donor motif monomer for photocatalytic hydrogen evolution from water. *J. Mater. Chem. A* **2023**, *11*, 4007–4012.

69 Chen, L.; Furukawa, K.; Gao, J.; Nagai, A.; Nakamura, T.; Dong, Y.; Jiang, D. Photoelectric covalent organic frameworks: converting open lattices into ordered donor–acceptor heterojunctions. *J. Am. Chem. Soc.* **2014**, *136*, 9806–9809.

70 Li, H.; Shao, P.; Chen, S.; Li, G.; Feng, X.; Chen, X.; Zhang, H. J.; Lin, J.; Jiang, Y. B. Supramolecular alternating donor–acceptor assembly toward intercalated covalent organic frameworks. *J. Am. Chem. Soc.* **2020**, *142*, 3712–3717.

71 Gottwald, F.; Penschke, C.; Saalfrank, P. Water splitting at imine-linked covalent organic frameworks. *Phys. Chem. Chem. Phys.* **2024**, *26*, 21821–21831.

72 Shi, T.; Wang, H.; Li, L.; Zhao, Z.; Wang, C.; Zhang, X.; Xie, Y. Enhanced photostability in protonated covalent organic frameworks for singlet oxygen generation. *Matter* **2022**, *5*, 1004–1015.

73 Li, X.; Pang, H.; Zhu, Y.; Xiang, Y.; Hu, J.; Huang, D. Enhanced protonation ability of covalent organic frameworks via N,O-bidentate chelation for photocatalytic H_2 evolution. *Chem. Commun.* **2024**, *60*, 1782–1785.

74 Zhao, Y.; Liang, Y.; Wu, D.; Tian, H.; Xia, T.; Wang, W.; Xie, W.; Hu, X.; Tian, X.; Chen, Q. Ruthenium complex of sp^2 carbon-conjugated covalent organic frameworks as an efficient electrocatalyst for hydrogen evolution. *Small* **2022**, *18*, 2107750.

75 Ye, H.; Gong, N.; Cao, Y.; Fan, X.; Song, X.; Li, H.; Wang, C.; Mei, Y.; Zhu, Y. Insights into the role of protonation in covalent triazine framework-based photocatalytic hydrogen evolution. *Chem. Mater.* **2022**, *34*, 1481–1490.

76 Dong, P.; Xu, X.; Wu, T.; Luo, R.; Kong, W.; Xu, Z.; Yuan, S.; Zhou, J.; Lei, J. Stepwise protonation of three-dimensional covalent organic frameworks for enhancing hydrogen peroxide photosynthesis. *Angew. Chem. Int. Ed.* **2024**, *63*, e202405313.

77 Yang, J.; Acharjya, A.; Ye, M.-Y.; Rabeah, J.; Li, S.; Kochovski, Z.; Youk, S.; Roeser, J.; Grüneberg, J.; Penschke, C.; Schwarze, M.; Wang, T.; Lu, Y.; Krol, R.; Oschatz, M.; Schomäcker, R.; Saalfrank, P.; Thomas, A. Protonated imine-linked covalent organic frameworks for photocatalytic hydrogen evolution. *Angew. Chem. Int. Ed.* **2021**, *60*, 19797–19803.

78 Ascherl, L.; Evans, E.W.; Gorman, J.; Orsborne, S.; Bessinger, D.; Bein, T.; Friend, R.H.; Auras, F. Perylene-based covalent organic frameworks for acid vapor sensing. *J. Am. Chem. Soc.* **2019**, *141*, 15693–15699.

79 Gao, X.; Yuan, J.; Wei, P.; Dong, J.; Chang, L.; Huang, Z.; Zheng, H.; Liu, J.; Jia, J.; Luan, T.; Zhou, B.; Yu, H.; Peng, C. Rational regulation of the exciton effect of acrylonitrile-linked covalent organic framework toward boosting visible-light-driven hydrogen evolution. *ACS Catal.* **2024**, *14*, 533–546.

80 Li, S.; Geng, Y.; Teng, B.; Xu, S.; Petkov, P.S.; Liao, Z.; Jost, B.; Liu, Y.; Feng, X.; Wu, B.; Zhang, T. Nature-inspired pyrylium cation-based vinylene-linked two-dimensional covalent organic framework for efficient sunlight-driven water purification. *Chem. Mater.* **2023**, *35*, 1594–1600.

81 Dai, L.; Dong, A.; Meng, X.; Liu, H.; Li, Y.; Li, P.; Wang, B. Enhancement of visible-light-driven hydrogen evolution activity of 2D π-conjugated bipyridine-based covalent organic

frameworks via post-protonation. *Angew. Chem. Int. Ed.* **2023**, *62*, e202300224.
82 Li, Q.; Wen, C.; Yang, J.; Zhou, X.; Zhu, Y.; Zheng, J.; Cheng, G.; Bai, J.; Xu, T.; Ji, J.; Jiang, S.; Zhang, L.; Zhang, P. Zwitterionic biomaterials. *Chem. Rev.* **2022**, *122*, 17073−17154.
83 Han, L.; Li, Y.; Yang, Y.; Sun, S.; Li, M.; Yue, J.; Chuah, C.Y.; Li, J. Zwitterionic covalent organic framework as a multifunctional sulfur host toward durable lithium-sulfur batteries. *J. Colloid Interface Sci.* **2022**, *628*, 144−153.
84 Ji, H.; Qiao, D.; Yan, G.; Dong, B.; Feng, Y.; Qu, X.; Jiang, Y.; Zhang, X. Zwitterionic and hydrophilic vinylene-linked covalent organic frameworks for efficient photocatalytic hydrogen evolution. *ACS Appl. Mater. Interfaces* **2023**, *15*, 37845−37854.
85 Zhang, Z.; Xu, Y. Hydrothermal synthesis of highly crystalline zwitterionic vinylene-linked covalent organic frameworks with exceptional photocatalytic properties. *J. Am. Chem. Soc.* **2023**, *145*, 25222−25232.
86 Wang, J.; Cao, Q.; Cheng, X.-F.; Ye, W.; He, J.-H.; Lu, J.-M. Moisture-insensitive and highly selective detection of no_2 by ion-in-conjugation covalent organic frameworks. *ACS Sens.* **2022**, *7*, 3782−3789.
87 Ben, H.; Yan, G.; Liu, H.; Ling, C.; Fan, Y.; Zhang, X. Local spatial polarization induced efficient charge separation of squaraine-linked COF for enhanced photocatalytic performance. *Adv. Funct. Mater.* **2022**, *32*, 2104519.
88 Ding, N.; Zhou, T.; Weng, W.; Lin, Z.; Liu, S.; Maitarad, P.; Wang, C.; Guo, J. Multivariate synthetic strategy for improving crystallinity of zwitterionic squaraine-linked covalent organic frameworks with enhanced photothermal performance. *Small* **2022**, *18*, 2201275.
89 Wang, H.; Qian, C.; Liu, J.; Zeng, Y.; Wang, D.; Zhou, W.; Gu, L.; Wu, H.; Liu, G.; Zhao, Y. Integrating suitable linkage of covalent organic frameworks into covalently bridged inorganic/organic hybrids toward efficient photocatalysis. *J. Am. Chem. Soc.* **2020**, *142*, 4862−4871.
90 Chen, C.; Xiong, Y.; Zhong, X.; Lan, P.C.; Wei, Z.; Pan, H.; Su, P.; Song, Y.; Chen, Y.; Nafady, A.; Sirajuddin; Ma, S.; Enhancing photocatalytic hydrogen production via the construction of robust multivariate Ti-MOF/COF composites. *Angew. Chem. Int. Ed*. **2022**, *134*, e202114071.
91 Xu, M.; Lu, M.; Qin, G.; Wu, X.; Yu, T.; Zhang, L.; Li, K.; Cheng, X.; Lan, Y. Piezo-photocatalytic synergy in $BiFeO_3$ @COF Z-scheme heterostructures for high-efficiency overall water splitting. *Angew. Chem. Int. Ed.* **2022**, *61*, e202210700.
92 Yu, S.; Li, C.; Lin, Y.; Zhang, J.; Liu, Y.; Yu, F. Interfacial N-Ti bond modulated COFs-TiO_2 type-II heterojunctions with directional charge transfer for efficient photocatalytic uranium reduction. *Sep. Purif. Technol.* **2024**, *341*, 126888.
93 Zhang, M.; Lu, M.; Lang, Z.-L.; Liu, J.; Liu, M.; Chang, J.-N.; Li, L.-Y.; Shang, L.-J.; Wang, M.; Li, S.-L.; Lan, Y.-Q. Semiconductor/covalent-organic-framework Z-Scheme heterojunctions for artificial photosynthesis. *Angew. Chem. Int. Ed.* **2020**, *59*, 6500−6506.
94 Ma, X.; Li, S.; Gao, Y.; Li, N.; Han, Y.; Pan, H.; Bian, Y.; Jiang, J. S-scheme heterojunction fabricated from covalent organic framework and quantum dot for enhanced photosynthesis of hydrogen peroxide from water and air. *Adv. Funct. Mater.* **2024**, *34*, 2409913.
95 Yuan, G.; Tan, L.; Wang, P.; Wang, Y.; Wang, C.; Yan, H.; Wang, Y.-Y. MOF-COF composite photocatalysts: design, synthesis, and mechanism. *Cryst. Growth Des.* **2022**, *22*, 893−908.
96 Zhang, L.; Zhang, J.; Yu, H.; Yu, J. Emerging S-scheme photocatalyst. *Adv. Mater.* **2022**, *34*, 2107668.
97 Elewa, A.M.; EL-Mahdy, A.F.M.; Hassan, A.E.; Wen, Z.; Jayakumar, J.; Lee, T.-L.; Ting, L.-Y.; Mekhemer, I.M.A.; Huang, T.-F.; Elsayed, M.H. Solvent polarity tuning to enhance the crystallinity of 2D-covalent organic frameworks for visible-light-driven hydrogen generation. *J. Mater. Chem. A* **2022**, *10*, 12378−12390.
98 An, Z.; Wu, C.Q.; Sun, X. Dynamics of photogenerated polarons in conjugated polymers. *Phys. Rev. Lett.* **2004**, *93*, 216407.
99 Zhou, T.; Wang, L.; Huang, X.; Unruangsri, J.; Zhang, H.; Wang, R.; Song, Q.; Yang, Q.; Li, W.; Wang, C.; Takahashi, K.; Xu, H.; Guo, J. PEG-stabilized coaxial stacking of two-dimensional covalent organic frameworks for enhanced photocatalytic hydrogen evolution. *Nat. Commun.* **2021**, *12*, 3934.
100 Jain, C.; Kushwaha, R.; Rase, D.; Shekhar, P.; Shelke, A.; Sonwani, D.; Ajithkumar, T.G.; Vinod, C.P.; Vaidhyanathan, R. Tailoring COFs: transforming nonconducting 2D layered COF into a conducting quasi-3D architecture via interlayer knitting with polypyrrole. *J. Am. Chem. Soc.* **2024**, *146*, 487−499.
101 Deng, M.; Chakraborty, J.; Wang, G.; Rawat, K.S.; Bourda, L.; Sun, J.; Nath, I.; Ji, Y.; Geiregat, P.; Van Speybroeck, V. V.; Feng, X.; Voort, P.V.D. Transforming 2D imine into 3D thiazole covalent organic frameworks by conjugated connectors: fully conjugated photocatalysts. *J. Am. Chem. Soc.* **2025**, *147*, 10219−10230.
102 Huang, Q.-Q.; Li, N.; Han, M.-S.; Liu, J.; Lan, Y.-Q. Conductive knitting of covalent organic framework manipulates spin density, orbital reorganization, and charge mobility for outstanding photoreactivity. *Angew. Chem. Int. Ed.* **2025**, *64*, e202513848.
103 Zhang, J.; Hu, W.; Cao, S.; Piao, L. Recent progress for hydrogen production by photocatalytic natural or simulated seawater splitting. *Nano Res.* **2020**, *13*, 2313−2322.
104 Zhao, J.; Ren, J.; Zhang, G.; Zhao, Z.; Liu, S.; Zhang, W.; Chen, L. Donor-acceptor type covalent organic frameworks. *Chem. Eur. J* **2021**, *27*, 10781−10797.
105 Liu, M.; Xu, Q.; Zeng, G. Ionic covalent organic frameworks in adsorption and catalysis. *Angew. Chem. Int. Ed.* **2024**, *63*, e202404886.
106 Zhang, P.; Wang, Z.; Cheng, P.; Chen, Y.; Zhang, Z. Design and application of ionic covalent organic frameworks. *Coord. Chem. Rev.* **2021**, *438*, 213873.
107 Zhang, T.; Jiang, Z.; Rappe, A.M. Hydrogenation of covalent organic framework induces conjugated π bonds and electronic topological transition to enhance hydrogen evolution catalysis. *J. Am. Chem. Soc.* **2024**, *146*, 15488−15495.
108 Liu, C.; Ding, R.; Yang, J.; Liu, S.; Chen, L.; Xu, Q.; Li, J.; Yin, X. Low-voltage hydrogen peroxide electrolyzer for highly efficient power-to-hydrogen conversion. *ACS Sustain. Chem. Eng.* **2023**, *11*, 2599−2606.
109 Feng, J.; Wei, Y.; Li, X.; Wang, Q.; Wang, B.; Guo, Y.; Feng, B.; Jin, E.; Yu, J. 3D-printed COF/Zeolite composites for augmented photocatalytic hydrogen peroxide production. *Angew. Chem. Int. Ed*. **2025**, *64*, e202508226.
110 Su, Y.; Li, B.; Xu, H.; Lu, C.; Wang, S.; Chen, B.; Wang, Z.; Wang, W.; Otake, K.; Kitagawa, S.; Huang, L.; Gu, C. Multi-component synthesis of a buta-1,3-diene-linked covalent organic framework. *J. Am. Chem. Soc.* **2022**, *144*, 18218−18222.
111 Yang, Y.; Niu, H.; Xu, L.; Zhang, H.; Cai, Y. Triazine functionalized fully conjugated covalent organic framework for efficient photocatalysis. *Appl. Catal., B* **2020**, *269*, 118799.
112 Wang, Z.; Yang, J.; Cao, J.; Chen, W.; Wang, G.; Liao, F.; Zhou, X.; Zhou, F.; Li, R.; Yu, Z.-Q.; Zhang, G.; Duan, X.; Wu, Y. Room-temperature synthesis of single iron site by electrofiltration for photoreduction of CO_2 into tunable syngas. *ACS Nano* **2020**, *14*, 6164−6172.
113 Zhao, J.; Shi, R.; Waterhouse, G.I.N.; Zhang, T. Selective photothermal CO_2 reduction to CO, CH_4, alkanes, alkenes over bimetallic alloy catalysts derived from layered double

hydroxide nanosheets. *Nano Energ.* **2022**, *102*, 107650.
114 Zhang, C.-R.; Cui, W.-R.; Yi, S.-M.; Niu, C.-P.; Liang, R.-P.; Qi, J.-X.; Chen, X.-J.; Jiang, W.; Liu, X.; Luo, Q. X.; Qiu, J. D. An ionic vinylene-linked three-dimensional covalent organic framework for selective and efficient trapping of ReO_4^- or $^{99}TcO_4^-$. *Nat Commun* **2022**, *13*, 7621.
115 Stegbauer, L.; Schwinghammer, K.; Lotsch, B.V. A Hydrazone-based covalent organic framework for photocatalytic hydrogen production. *Chem. Sci.* **2014**, *5*, 2789–2793.
116 Liu, Y.; Gong, C.; Wang, R.; Guo, J.; Li, J.; Wang, Q.; Lv, Z.; Ling, T. High-performance neutral Zn–air batteries: revolutionizing energy storage with concurrent hydrogen peroxide electrosynthesis. *Green Chem.* **2025**, *27*, 11144–11154.
117 Chen, Y.; Zaman, F.; Jia, Y.; Huang, Y.; Li, T.; Bai, F.; Li, L.; Song, L.; Li, J. Harmful cyanobacterial bloom control with hydrogen peroxide: mechanism, affecting factors, development, and prospects. *Curr. Pollut. Rep.* **2024**, *10*, 566–579.
118 Rigoletto, M.; Laurenti, E.; Tummino, M.L. An overview of environmental catalysis mediated by hydrogen peroxide. *Catalysts* **2024**, *14*, 267.
119 Bailey, D.; Rizk, E.B. Origin and use of hydrogen peroxide in neurosurgery. *Neurosurgery* **2021**, *89*, E3.
120 Ma, S.; Deng, T.; Li, Z.; Zhang, Z.; Jia, J.; Li, Q.; Wu, G.; Xia, H.; Yang, S.; Liu, X. Photocatalytic hydrogen production on a sp^2-carbon-linked covalent organic framework. *Angew. Chem. Int. Ed.* **2022**, *61*, e202208919.
121 Hou, Y.; Zhou, P.; Liu, F.; Lu, Y.; Tan, H.; Li, Z.; Tong, M.; Ni, J. Efficient photosynthesis of hydrogen peroxide by cyano-containing covalent organic frameworks from water, air and sunlight. *Angew. Chem. Int. Ed.* **2024**, *63*, e202318562.
122 Di, X.; Lv, X.; Wang, H.; Chen, F.; Wang, S.; Zheng, G.; Wang, B.; Han, Q. Enhanced pre-sensitization in metal-free covalent organic frameworks promoting hydrogen peroxide photosynthesis. *Chem. Eng. J.* **2023**, *455*, 140124.
123 Zhang, B.; Wei, M.; Mao, H.; Pei, X.; Alshmimri, S. A.; Reimer, J.A.; Yaghi, O.M. Crystalline dioxin-linked covalent organic frameworks from irreversible reactions. *J. Am. Chem. Soc.* **2018**, *140*, 12715–12719.
124 Yu, Z.; Yu, F.; Xu, M.; Feng, S.; Qiu, J.; Hua, J. Amidoxime-functionalized sp^2-carbon-conjugated covalent organic frameworks for overall photocatalytic hydrogen peroxide production. *Adv. Sci.* **2025**, *12*, 2415194.
125 Wang, X.; Li, H.; Zhou, S.; Ning, J.; Wei, H.; Li, X.; Wang, S.; Hao, L.; Cao, D. Donor–acceptor fully sp^2-carbon conjugated covalent organic frameworks for photocatalytic H_2O_2 production. *Adv. Funct. Mater*. **2025**, 2424035.
126 Chi, X.; Zhang, Z.; Li, M.; Jiao, Y.; Li, X.; Meng, F.; Xue, B.; Wu, D.; Zhang, F. Vinylene-linking of polycyclic aromatic hydrocarbons to π-extended two-dimensional covalent organic framework photocatalyst for H_2O_2 synthesis. *Angew. Chem. Int. Ed.* **2025**, *64*, e202418895.
127 Xiong, X.; Zhao, Y.; Shi, R.; Yin, W.; Zhao, Y.; Waterhouse, G.I.N.; Zhang, T. Selective photocatalytic CO_2 reduction over Zn-based layered double hydroxides containing tri or tetravalent metals. *Sci. Bull.* **2020**, *65*, 987–994.
128 Lin, H.; Liu, Y.; Wang, Z.; Ling, L.; Huang, H.; Li, Q.; Cheng, L.; Li, Y.; Zhou, J.; Wu, K.; Zhang, J.; Zhou, T. Enhanced CO_2 photoreduction through spontaneous charge separation in end-capping assembly of heterostructured covalent-organic frameworks. *Angew. Chem. Int. Ed.* **2022**, *61*, e202214142.
129 Yang, N.; Yan, W.; Zhou, Z. J.; Tian, C.; Zhang, P.; Liu, H.; Wu, X. P.; Xia, C.; Dai, S.; Zhu, X. Synthetic leaves based on crystalline olefin-linked covalent organic frameworks for efficient CO_2 photoreduction with water. *Nano Lett.* **2024**, *24*, 5444–5452.
130 Li, G.; Fu, Y.; Zhang, Z. F.; Chen, D.; Feng, L.; Zhou, J.; Zhang, Y.; Zhou, Z.; Su, Z. Tailoring 3D COFs with vinyl motifs boosts intramolecular electron transfer for photocatalytic CO_2 reduction to HCOOH. *Sep. Purif. Technol.* **2025**, *376*, 134002.
131 Wang, W.; Zhang, X.; Lv, G.; Yan, T.; Li, J.; Huang, H. Creating direct interlayer charge transport channels in vinyl-linked 2D covalent organic framework for efficient photocatalytic CO_2 reduction. *Appl. Catal. B Environ. Energy* **2025**, *372*, 125299.
132 Liu, Y.; Wang, Y.; Shang, J.; Peng, J.; Zhu, T. Construction of a novel metal-free heterostructure photocatalyst PRGO/TP-COF for enhanced photocatalytic CO_2 reduction. *Appl. Catal. B Environ.* **2024**, *350*, 123937.
133 Cheng, Y. Z.; Ji, W.; Hao, P. Y.; Qi, X. H.; Wu, X.; Dou, X. M.; Bian, X. Y.; Jiang, D.; Li, F. T.; Liu, X. F.; Yang, D. H.; Ding, X.; Han, B. A fully conjugated covalent organic framework with oxidative and reductive sites for photocatalytic carbon dioxide reduction with water. *Angew. Chem. Int. Ed.* **2023**, *62*, e202308523.
134 Tao, F.; Zhou, W.; Li, Z.; Jiang, X.; Wang, L.; Yu, Z.; Zhang, J.; Zhou, H. Regulating donor–acceptor interactions within 2-methylpyridine-mediated vinylene-linked covalent–organic frameworks for enhanced photocatalysis. *ACS Mater. Lett.* **2024**, *6*, 1120–1129.
135 Wang, W.; Wang, H.; Tang, X.; Huo, J.; Su, Y.; Lu, C.; Zhang, Y.; Xu, H.; Gu, C. Phenothiazine-based covalent organic frameworks with low exciton binding energies for photocatalysis. *Chem. Sci.* **2022**, *13*, 8679–8685.
136 Zhang, J.; Tao, F.; Wang, W.; Gong, C.; Li, Z.; Zhou, W.; Peng, Y.; Zhou, H. Isoreticular series of 2-methylpyridine-mediated vinylene-linked covalent organic frameworks for efficient visible-light-driven thiocyanation. *ACS Mater. Lett.* **2023**, *5*, 2799–2806.
137 Zhao, Y.; Liu, H.; Wu, C.; Zhang, Z.; Pan, Q.; Hu, F.; Wang, R.; Li, P.; Huang, X.; Li, Z. Fully conjugated two-dimensional sp^2-carbon covalent organic frameworks as artificial photosystem I with high efficiency. *Angew. Chem. Int. Ed.* **2019**, *58*, 5376–5381.
138 Zhang, F.; Dong, X.; Wang, Y.; Lang, X. Design and synthesis of a triazine-based sp^2 carbon-conjugated covalent organic framework for blue light photocatalysis. *Small* **2023**, *19*, 2302456.
139 He, T.; On, I.K.W.; Bi, S.; Huang, Z.; Guo, J.; Wang, Z.; Zhao, Y. Crystalline olefin-linked chiral covalent organic frameworks as a platform for asymmetric catalysis. *Angew. Chem. Int. Ed.* **2024**, *63*, e202405769.
140 Wang, W.; Cai, K.; Zhou, W.; Tao, F.; Li, Z.; Lin, Q.; Wang, L.; Yu, Z.; Zhang, J.; Zhou, H. Nanoporous vinylene-linked 2D covalent organic frameworks for visible-light-driven aerobic oxidation. *ACS Appl. Nano Mater.* **2023**, *6*, 8396–8403.
141 Li, M.; Chi, X.; Zhang, Z.; Bi, S.; Meng, F.; Jiao, Y.; Mou, K.; Wang, Z.; Xue, B.; Li, X.; Zhang, F. Mesoporous vinylene-linked covalent organic frameworks with heteroatom-tuned crystallinity and photocatalytic behaviors. *Angew. Chem. Int. Ed.* **2024**, *63*, e202411474.
142 Li, Z.; Wang, W.; Tao, F.; Zhou, W.; Wang, L.; Yu, Z.; Wang, K.; Zhang, J.; Zhou, H. Fabricating *s*-collidine-derived vinylene-linked covalent organic frameworks for photocatalysis. *Chem. Commun.* **2023**, *59*, 11728–11731.
143 Jin, C.; Pang, Y.; Wang, R.; Wu, S.; He, H.; Gao, L.; Liu, J.; Chen, L.; Li, Y.; Yan, X.; Wang, B. Thiophene-based vinylene-linked donor-acceptor covalent organic frameworks for photocatalytic organic transformations. *Appl. Catal., A* **2024**, *685*, 119906.
144 Bi, S.; Zhang, Z.; Meng, F.; Wu, D.; Chen, J.; Zhang, F. Heteroatom-embedded approach to vinylene-linked covalent organic frameworks with isoelectronic structures for photoredox catalysis. *Angew. Chem. Int. Ed.* **2022**, *61*, e202111627.
145 Zhang, Z.; Bi, S.; Meng, F.; Li, X.; Li, M.; Mou, K.; Wu, D.; Zhang, F.

Hexatopic vertex-directed approach to vinylene-linked covalent organic frameworks with heteroporous topologies. *J. Am. Chem. Soc.* **2023**, *145*, 16704−16710.
146 Yu, F.; Li, C.; Li, W.; Yu, Z.; Xu, Z.; Liu, Y.; Wang, B.; Na, B.; Qiu, J. Π-skeleton tailoring of olefin-linked covalent organic frameworks achieving low exciton binding energy for photo-enhanced uranium extraction from seawater. *Adv. Funct. Mater.* **2024**, *34*, 2307230.
147 Xu, Y.; Yu, Z.; Zhang, Q.; Luo, F. Sulfonic-pendent vinylene-linked covalent organic frameworks enabling benchmark potential in advanced energy. *Adv. Sci.* **2023**, *10*, 2300408.
148 Zhong, L.; Feng, X.; Zhang, Q.; Xie, X.; Luo, F. An imidazole-based covalent-organic framework enabling a super-efficiency in sunlight-driven uranium extraction from seawater. *Chem. Sci.* **2024**, *15*, 10882−10891.
149 Cui, W. R.; Zhang, C. R.; Xu, R. H.; Chen, X. R.; Yan, R. H.; Jiang, W.; Liang, R. P.; Qiu, J. D. High-efficiency photoenhanced extraction of uranium from natural seawater by olefin-linked covalent organic frameworks. *ACS EST Water* **2021**, *1*, 440−448.
150 Zhao, Y.; Li, S.; Fu, G.; Yang, H.; Li, S.; Wu, D.; Zhang, T. Construction of layer-blocked covalent organic framework heterogenous films via surface-initiated polycondensations with strongly enhanced photocatalytic properties. *ACS Cent. Sci.* **2024**, *10*, 775−781.
151 Han, J.; Zhang, T. The emerging of 2D layer-blocked frameworks. *ChemCatChem* **2025**, *17*, e202401320.

https://doi.org/10.1007/s10118-025-3550-0